INTELLIGENT GRIPPER, WITH MULTI-SENSOR FINGER PAD, FOR THE SARCOS DEXTROUS ARM

by

Ping Zhang

Department of Electrical Engineering

Center for Intelligent Machines

McGill University

Montréal, Québec

Canada

January 1999

A DISSERTATION

SUBMITTED TO THE FACULTY OF GRADUATE STUDIES AND RESEARCH

OF MCGILL UNIVERSITY

IN PARTIAL FULFILLMENT OF THE REQUIREMENTS FOR

THE DEGREE OF MASTER OF ENGINEERING

Abstract

This thesis presents the Intelligent Gripper, a low cost instrumented robot finger pad which is equipped with an 8 × 8 tactile sensing array and a 2 × 2 proximity sensing grid. The complete system is composed of three modules. The capacitive tactile sensing array utilizes a dual strip construction to improve its robustness and simplicity, a technology initially developed by Sarcos Research Inc. The proximity network is based on infrared range sensing technology. The microprocessor based interface module gives the system intelligent capability. In order to reduce the noise and to improve the system modularity, all electric circuitry is localized. The modular architecture gives the system excellent portability.

Following the comprehensive evaluation and characterization of the tactile sensing array and its associated electronic system, an experimental exploration to use the tactile sensor in transient contact force control is presented. It is found that using feedback from tactile sensor stabilizes the force control. However, the highest performance for transient force control is achieved from a combined feedback from tactile sensor and joint force sensor.

Résumé

Cette thèse présente une préhenseur intelligente, une garniture des doigts robotiques, équipée d'une matrice (8×8) de capteurs tactile et une grille (2×2) des capteurs de proximité. C'est une design economique et très portable. La matrice tactile capacitif est basée sur la technologie dévelopé initialement par Sarcos Research Inc., il est de construction de bande duelle pour améliorer sa robustesse et simplicité. La réseau de proximité emploie la technique mesurant dans la limite d'infrarouge. Un module d'interface à base de microprocesseur donne au système la capacité intelligente. Pour réduire le bruit et pour améliorer la modularité du système, tous les circuits électriques sont localisés.

Après l'évaluation et la caractérisation complètes de matrice tactile et de son système électronique associé, une exploration expérimentale d'utiliser le capteur tactile dans la commande de force de contact passagière est présentée. On constate que l'utilisation du feedback tactile stabilise la commande de force. De plus, un combinaison de capteur tatcile et capteur joint force donne le meilleur performance pour la commande de force d'impact.

Acknowledgements

I would like first and foremost to express my gratitude to my supervisor, Professor John M. Hollerbach, whose support and encouragement were indispensable throughout my master's program. He contributed a great deal of his time, effort and thought to the work presented in this dissertation. Professor Hollerbach showed dedication to his students and his profession. During the years of my study in the program, I also received generous financial support from him, without which it would be impossible for me to complete this program. I consider myself fortunate to have been working in association with him.

I would also like to express my gratitude to Professor Martin Buehler and Doctor Yangming Xu. Professor Buehler dedicated a large amount of time on many technical details and gave numerous valuable comments. Without his contribution, this thesis would not be completed. Doctor Xu had been my mentor through out the years when I was working in Biorobotics Lab. It was a great pleasure to work with him because of his brilliant intelligence and great personality.

I am grateful to the Center for Intelligent Machines and IRIS, and the Center for Engineering Design, University of Utah for their financial and material support. Thanks to Sarcos Research Inc. for allowing me to use their initial technology and facilities to develop the tactile sensor. Special thanks should go to David Johnston of Sarcos for his comprehensive help and constructive suggestions. Without his efforts, most of the experiments would not be possible or conclusive.

I wish to thank all my colleagues and friends during my years with Biorobotics Lab both at McGill University and at University of Utah. Special mention should be made of Ali Nahvi, Zhiling Qiu and Donghai Ma.

Finally, I give my thanks to my wife, Xiaoyan, for her constant support through the years and for the cheer and love we share in the family.

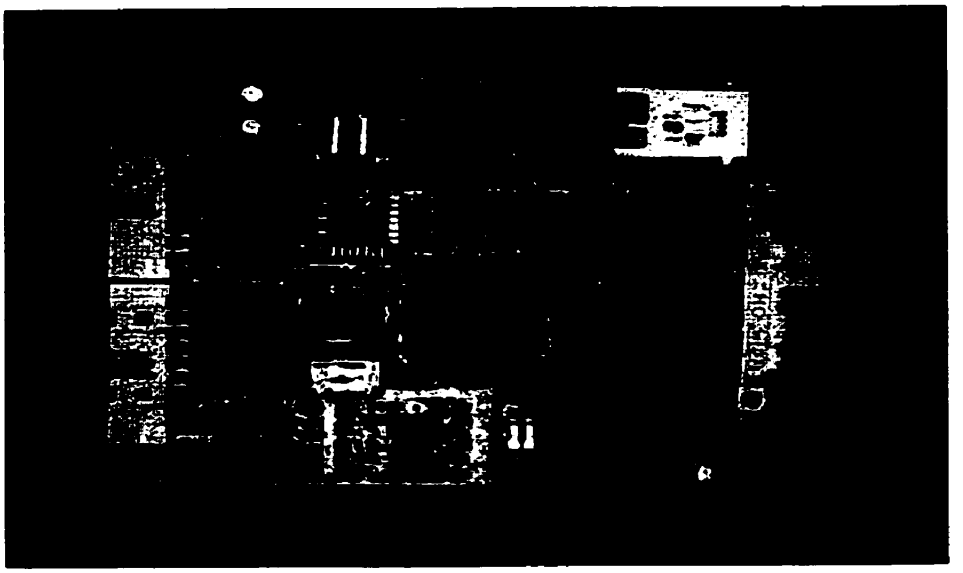

Figure 0.1: Interface module PCB

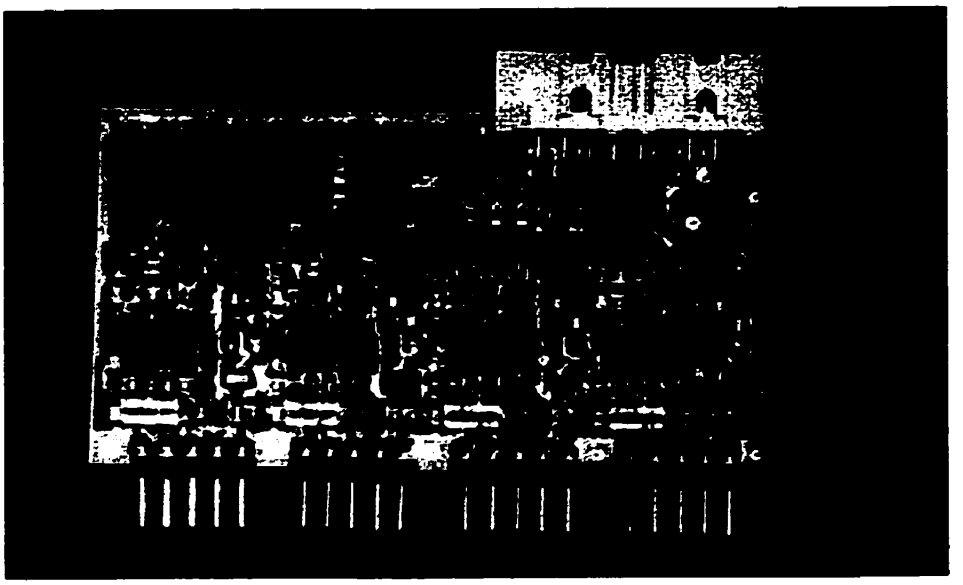

Figure 0.2: Proximity sensing subsystem PCB

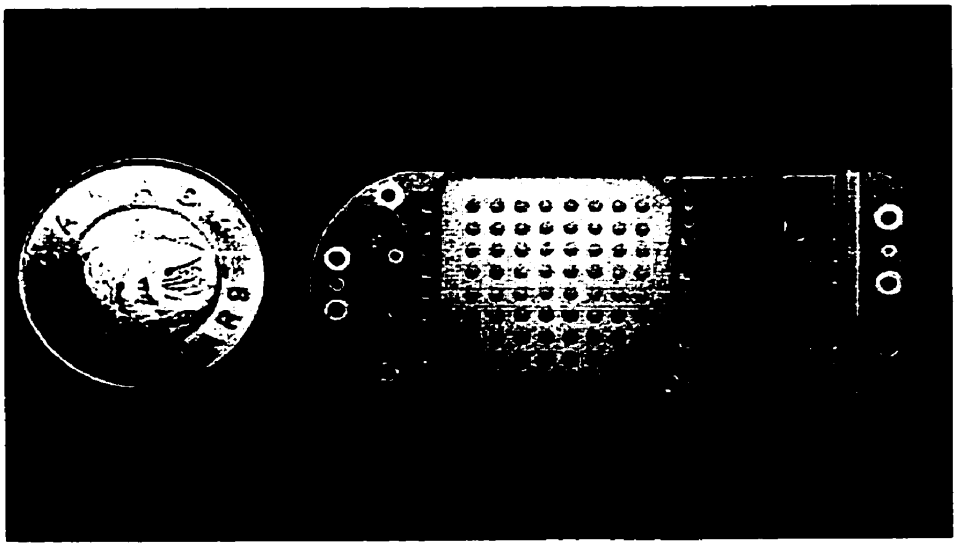

Figure 0.3: Tactile subsystem (top view): tactile array and back PCB

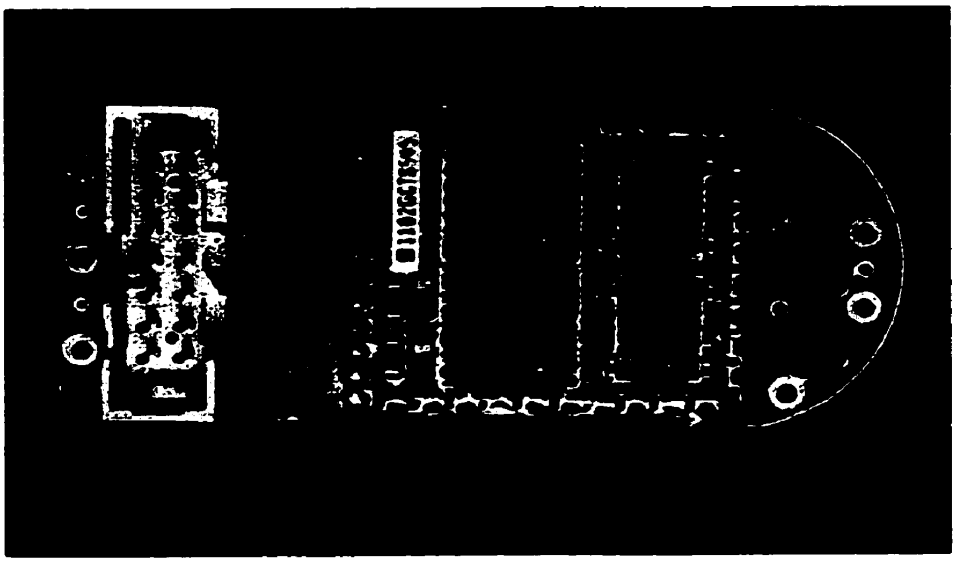

Figure 0.4: Tactile subsystem (bottom view): localized circuitry and back PCB

Contents

List of Tables

List of Figures

Chapter 1

Introduction

1.1 Motivation and Review

In recent years we have been witnessing implementation of automated handling machines in various scientific research and industry manufacturing environments. While automation and robotics are becoming a matter of routine in our modern industrialized society we need a wide spread of robots and associated hardware and software. To meet with these requirements, precise data must be provided as fuel for the information processing. These goals will partly be achieved if cheap, reliable and easily implementable sensor systems are introduced.

Adding sensing capability to a robot end-effector provides the robot with intelligent perception capability and flexibility of decision making. To perform intelligent tasks, robots are highly required to perceive their operating environment, and react accordingly. With this regard, tactile sensors and proximity sensors offer to extend the scope of intelligence of a robot for performing tasks which require object recognition, touching and manipulation. The goal is to develop an intelligent robotic manipulator which is able to "see and feel" and make the decisions based on the knowledge acquired from its sensing system.

1.1.1 Tactile Sensing

Tactile sensors provide a sense of touch similar to the human hand by measuring the local distribution of forces on the surface. A dextrous robot gripper needs to determine the position of the objects to reliably grasp and manipulate them and tactile sensors are capable to supply these most useful parameters. Therefore the autonomous robotic manipulation is probably the most important application for tactile sensors.

In a simple grasping task, the manipulator needs to be controlled so that the object position relative to end-effector changes from point contact to line contact and then to a plane contact. The utilization of sensory feedback from tactile and force/torque sensors makes this process possible. After an initial contact, the object is rotated around the gripper approach vector until the object makes a line contact with the surface. The angle between the gripper held object and the surface is then calculated from tactile sensory information. The position and orientation of the gripper are modified based on the current gripper position and the orientation, and the angle calculated so as to place the object on the plane.

As an example, Reynaerts and Van Brussel [RVB93] demonstrated a method for fully envelope rolling manipulation using a robot hand with an index finger and a thumb, both driven by tendon. The method is using tactile information to estimate the contact circumstances with the local curvature of the object. A two dimensional model for object manipulation is proposed based on the study of the movement of the contact lines between the index and the thumb.

By characterizing the dynamic forces on a tactile sensor array, it is possible to extract a tactile image during a grasping or a releasing operation. This process provides more intelligent capability to the robotic manipulator for object recognition and environmental perception. Berger and Kholsa [BK91] proposed a controller that utilizes the tactile sensor in the feedback loop to determine the location and the orientation of the object edge and surface, while Petriu Emil and McMath William [PMYT92] presented an experimental robotic system using a 16×16 tactile sensor array and an

instrumented compliant wrist developed specifically for the active perception of geometric profiles of the object surface. Rafla and Merat [RM90] developed a more sophisticated system with multiple sensing devices, a Vision-Traction Exploration (VTE) strategy for generating surface descriptions from range vision and tactile sensor data. The range vision system provides primary sparse 3-D data about the surface. With the use of tactile and force torque sensors under position control, supplementary data are obtained and processed. These two sets of data are integrated and processed in a higher level for precise surface representation and classification.

On the other hand, the control of the behavior of manipulators during gripper-object contact transient remains a big challenge due to the high non-linearity of the process. By integrating joint torque sensing and tactile sensor spatial and force information, it is possible to increase the sensitivity in measuring the applied force and contact locations, therefore improves the performance of the control. Using tactile sensors on a whole arm manipulator overcomes a number of limitations in the joint torque method due to insufficient or low accuracy measurements [GT89].

Tactile sensing is not only a powerful tool for intelligent robotic research and development, but also has great potentials in industry automation. A tactile sensor system, capable of providing pressure images of the objects which are held in a robot gripper, will be a very useful aid for programmable assembly tasks and will provide information which enables verification and correction of an assembly process.

While industrial robots have grown to be a major force in production lines, the positioning control type robot is difficult to be employed in the automation of assembly lines where the robot must deliver a delicately controlled force and at the same time adapts itself to the constraining conditions of workplaces. A robot needs the accurate description of the location of the parts to control the end effector. However, it is extremely difficult to improve absolute positioning accuracy [Asa86]. The tactile sensor and the compliance device can compensate for or absorb the relative errors between end-effector and work pieces.

1.1.2 Proximity Sensing

Cost-effective solutions to autonomous robot control and to the industry production problems through flexible automation require the ability to adapt to circumstances and tasks which could change with great frequency. An autonomous robot deals with the empirical world which is never fully predictable. While tactile sensing offers a solution to this issue, a proximity sensor is a non-touch alternative to physically actuated devices. In some cases where physical contact is hazardous a proximity sensor may be the only solution.

Proximity sensors are able to extract geometrical information about the surrounding environment and to perceive other relevant features of the selected objects. With proximity sensors, the robotic manipulator is able to construct a geometric model of the unknown environment without making physical contact with the environment.

Proximity sensors have two major applications – collision detection and object recognition. Real-time collision detection has an important role as part of a safety system in telerobotics and autonomous robotics application. The accurate sensing of its proximity sensor enhances the ability of an autonomous robotic manipulator to operate in confined spaces while avoiding unwanted collisions. Wegerif and Rosinski [Lee92] developed a sensor based obstacle avoidance strategy for a SCARA-type robot manipulator using infrared proximity sensors to provide real time knowledge of the environment surrounding the manipulator. The control algorithm produces a collision free path around detected obstacles based on proximity information, while allowing the end-effector to reach the desired goal position, and Novak and Feddema [NF92] addressed the issue of collision avoidance in unknown or partially modeled environments using a capacitive proximity sensor which can detect the obstacles up to 40 cm.

Similar to the tactile sensing, proximity sensors also can be used to identify the geometrical characters such as edge and surface profiles of the manipulated object in a non-contact fashion. Proximity sensors can become fingers, hands and even the

tactile control of critical and routine manufacturing and inspection process - from the power system maintenance, the pharmaceutical inspection and the food packaging to the manufacture of ships, automobiles, and airplanes in which case it is important to have the robot arm in precision tracking of the surface and the contour of an object. Lee [Lee92] proposed an optical proximity system, capable of measuring the distance to the orientation and the discontinuity at a local area of an object surface. Lee and Hahn [LH91] also used an optical proximity sensor system mounted on a robot end-effector for 3-D quadric objects identification.

1.1.3 The Goal

There are numerous tactile and proximity sensing devices of various type had been developed since these sensing concepts were discovered. However, almost all of the systems remain in the stage of laboratory prototype which are fragile, in-robust, and difficult to fabricate. Also, due to the large quantity of sensor units involved, they require significant processing power which can be very expensive. For example, a VME based real-time system with single CPU and general purpose analog I/O channels costs thousands of dollars. Though some systems with good performance have been developed, they are usually very expensive and only serve very specific scientific research purposes.

The rapid decline in the cost of information processing power brought about by the widespread availability of microprocessors and fast pace in discovery of innovative materials have driven forward the development of advanced sensing devices. It is possible now to bring a truly usable, robust and cheap system into reality. In this thesis, we propose and implement a compact sensing system, the Intelligent Gripper System, which integrates sensing arrays for both tactile and proximity with smart and user friendly functionality. The simplicity in the sensor fabrication process and the state-of-art electrical design assure it to be a product prototype. Though the system is primarily designed for Sarcos Dextrous Slave Arm, it can be easily adapted for other

robotic manipulators due to its modular and portable approach.

1.2 Author's contributions

The author proposed and successfully implemented an unique sensing system called Intelligent Gripper System for the Sarcos Dextrous Arm. The system which has been developed integrates a high performance 8×8 capacitive tactile sensing array and a 2×2 infrared photon-electronic proximity sensing array into a compact structure which can be installed on the finger tip of a manipulator.

While there might not be many challenges in the fundamental concepts for these sensors, the work is mainly devoted to simplify and standardize the tactile sensor fabrication procedure and to physically integrate the supporting electronics with both sensing subsystems using off-the-shelf components. The concept of a micro-controller based interface module which plays a role as a hub for both sensing systems and the master controller not only makes the sensor intelligent but also balances the processing load among resources of the entire system, therefore the performance of the control system of the manipulator is potentially improved. As a product prototype, this simple, robust, inexpensive and portable system with satisfactory performance is a good example which shows the long existing gap between laboratory prototype and commercial product can be eliminated with low cost.

On the other hand, a complete evaluation and characterization of the tactile sensing array is conducted through experiments and the results are presented. Furthermore, the author proposed a potential application of the system by suggesting a tactile sensor based transient force control strategy with supplemented joint force/torque information. The experiment results show that this strategy has a good performance and is an interesting topic for future research.

1.3 Organization of the Thesis

The thesis is organized into five chapters. As an introduction, the first chapter gives the background of tactile and proximity sensing in robotic manipulation and establishes the goal of this thesis. The second chapter illustrates principles of the capacitive tactile sensing devices as well as the design strategy and rules. A brief review of the sensing devices of various types is also presented. The design and implementation are described in chapter three with detailed figures and flow charts. In chapter four, two sets of experiments and their results are demonstrated, one for the evaluation and the characterization of the system developed and the other explores the feasibility of the tactile sensor based force control as well as its performance evaluation. Finally in chapter five the conclusion has been drawn followed by discussions. All the technical details are listed in appendixes for documentation.

Chapter 2

Strategy and Principle

2.1 System Specifications

The purpose of this thesis is to design and to implement a product prototype of the next generation gripper system for Sarcos Dextrous Slave Arm. In general, the entire design specification falls into two categories, the functionality and technical specifications.

2.1.1 Functionality

The Intelligent Gripper System integrates both tactile and proximity sensing devices and is designed to work with the Sarcos Dextrous Slave Arm.

During the past years, numerous tactile sensing devices adopting a broad range of principles and technologies have been developed [Dar89, HC92]. In summary, almost all of the tactile sensors are based on conductive, inductive, capacitive, photo-electric, magnetic, piezoelectric, electric-acoustic and silicone micromechanical principles. Uldry and Rusell [UR92] made a tactile sensor using compliant elastomer, a conductive rubber which changes conductivity under stress. Reston and Kolesar [RK89] developed a sensor from piezoelectric polyvinylidene fluoride while Bergamasco [FDB88] used piezoelectric polymer [PVF2] for the similar device. A photo-electric approach was reported by Schoenwald and Martin [SM] with good results. A magnetic type

tactile sensor array was developed by Vranish [Vra] but its spacing is 5mm which is relatively large. An ultrasonic emission tactile sensor was developed by Shinoda and Ando [SA94].

Tactile sensors using conductive elastomers are inexpensive and flexible. However, these materials suffer from problems including hysteresis, contact noise, fatigue, low sensitivity and nonlinear response [Hil82, Spe90]. Photo-electric tactile sensors tactile sensors using optical fibers yield considerable sensitivity and can be made very small. But they are very difficult to be packed into a modular device due to the presence of photonic components and circuitry. Piezo-electric tactile sensors and electro-acoustic tactile sensors based on similar materials have been used most often because of their flexibility, fast response, good sensitivity and ability to provide multi-dimensional sensing capability. However, they are either unable to measure static loads or too complicated to multiplex. Magnetic and inductive tactile sensing devices are able to sense shears as well as normal forces, but highly depend on the material properties of the operating environment to achieve satisfactory performance. Besides, they are not suitable to be implemented as arrays. Silicone micromechanical tactile sensors are tiny structures "machined" from wafers of silicone using integrated circuit fabrication techniques. Though they generally have very good sensing performance, these sensors are not suitable for human-sized manipulators. They are also very expensive in small quantity.

Capacitive tactile sensors have been popular with a number of research groups. They offers satisfactory performance and can be fabricated into curved fingertips which is essential for dexterous manipulation [Fea90]. Construction techniques are relatively simple and inexpensive, as are capacitive measurement and multiplexing electronics. It is the best solution to use capacitive tactile sensors for human-sized manipulators like the Sarcos Dextrous Arm.

There has been a number of publications on capacitive tactile sensing technology since early 80's. Boie [Boi84] developed a three-layer sandwich structure. The top layer

is columns of compliant metal strips over a central elastic dielectric sheet. The bottom layer is a flexible printed circuit board with rows of metal strips and multiplexing circuits. A readout of the capacitor values corresponds to a sampled tactile image. Fearing [Fea90, FB91] developed a similar device which embedded thin copper strips into the top layer. Siegel and Hollerbach [SGH86] developed a doped rubber conducting top layer, which was connected to by wires. To avoid problems with edge connection to the top strips, Jacobsen and McCammon [JMBP88, McC90, MJ90] proposed a structure using floating top electrodes.

Proximity sensors can be realized through broader span of principles and technologies including capacitive, inductive, magnetic, photon-electronic, laser interferometer, vision capturing, ultrasonic and much more. These devices can be very sophisticated and provide comprehensive proximity information with great accuracy, or as simple as a generic component with basic sensing capability. To achieve a compact design with low cost, a simple, robust proximity sensor is needed. The infrared LED/photo-transistor proximity sensor developed by Petryk and Buehler [PB96] is an excellent choice to fulfill this requirement. They also proved that this sensor has a good performance and application potential.

The Intelligent Gripper System is an accessory of an existing robot gripper. Therefore neither hardware nor software modification to the original gripper system should be allowed.

A robotic manipulator arm is typically controlled by a centralized computer, the master controller. Given a proximity sensor and a tactile sensor, we need an interface to exchange data between them and the master controller. Through this interface, the master controller can issue the configuration command to sensors and receive sensor readings from them. Though the Intelligent Gripper System is for the Sarcos Dextrous Slave Arm, it should also be able to work with other robot arms. To reduce the additional computation load on the central computer, the Intelligent Gripper System must have intelligent capabilities to perform all the low level data processing. Besides,

we require no hardware modifications when it is connected into or disconnected from the existing control system. Ideally, it should be a "plug and play" device. Therefore a simple, clean, and standard interface is mandatory. On the other hand, maintenance of a robotic system is a big headache especially to the scientific research community, the Intelligent Gripper System must be easy to use, easy to service, and it should have built-in tools for debugging and calibration.

In summary, the Intelligent Gripper System is a portable sensing system including a proximity sensing subsystem and a tactile array. The system is able to perform all the preliminary data processing and has a simple, clean and standard interface to the central computer. It also has built-in debugging tools.

2.1.2 Technical Specification

Sarcos Dextrous Slave

As an accessory, many of the specifications of the Intelligent Gripper System are identified according to its host, the Sarcos Dextrous Slave Arm.

The Sarcos Dextrous Slave Arm is a human-size robot arm with ten Degrees Of Freedom (DOF), made by Sarcos Research Inc. (390 Wakara Way, Salt Lake City, UT84108). It has three DOF for the shoulder, one DOF for the elbow and three DOF for the wrist. The Slave has one thumb with two DOF, one index finger with one DOF and an additional passive index finger. All joints are hydraulically driven. The joint torque sensor is standard equipment for all joints. All joints are equipped with joint encoders or RVDT's. Table 2.1 is the mechanical specifications of the three finger joints.

Specifications

For tactile arrays, it is a compromise between sensor density and implementability. As a low cost product prototype, it is realistic to have an 8×8 tactile array with $0.1in$ spacing. According to Table 2.1, the maximum torque of the rotational finger joint is

Joint Number	8	9	10
Function	Thumb	Thumb	Index
Actuator Type	Rotary	Rotary	Linear
Maximum Torque[in-lb]	450	450	100 N
Maximum Slew Rate[deg/sec]	200	200	8 in/sec
Range of Motion [deg]	90	90	3.5 in
Link Length [in]	5.0	5.0	5.0

Table 2.1: Mechanical specifications of the finger joints

$450in - lb$ which translates into $90lb$ maximum force on the finger tip, roughly $1.4lb$ on each tactile cell for an 8×8 array.

For proximity sensors, a 2×2 sensing array is adequate to give the position of the finger and the orientation of its normal vector, relative to the environment.

In summary, we want the Intelligent Gripper System to meet the following expectations.

Tactile Sensing Subsystem:	
Sensing Type:	Capacitive
Array Type:	Flat
Density:	8×8 with $0.1in$ spacing
Sensing Range:	$0 - 1.4lb$
Proximity Sensing Subsystem:	
Sensing Type:	Infrared LED/Photo-transistor pair
Array Type:	Flat
Density:	2×2
Sensing Range:	$0 - 5cm$
Supporting Electronics:	
Power Supply:	$5.0V$, $\leq 1.0A$
Sensor Resolution:	$8 - 12bit$
weight:	$\leq 1.0lb$ (suitable to be installed on the robot arm)
Interface:	One 8 bit parallel port, one RS-232 serial Port.

2.2 Tactile Sensing Principle

The Intelligent Gripper System uses capacitance based tactile sensing. Figure 2.1 shows the basic structure of a single tactile sensor unit, a tactile cell. It has three basic layers. The top is a moving plate and the bottom is a static plate, both are made from conductive material. Between them is a dielectric layer, usually silicone or air.

If A is the area of the plates and assuming the distance d between top and bottom plates is much smaller than their dimensions, the capacitance of the cell is:

$$C = \frac{\epsilon_0 \epsilon_r A}{d} \tag{2.1}$$

where $\epsilon_0 = 8.85 \times 10^{-12} Fm^{-1}$ is the permittivity and ϵ_r is the dielectric constant of

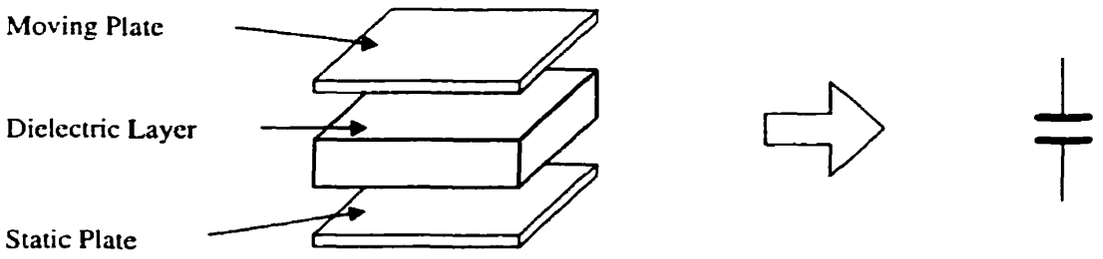

Figure 2.1: A single tactile cell

the dielectric layer.

When the external force is applied to the tactile cell, d is reduced therefore the capacitance is increased. By measuring this capacitance, the tactile information is extracted.

To measure the actual capacitance of a tactile cell, a high frequency AC voltage V is applied to the sensor. This is called excitation of the sensor. The AC current I which flows across the sensor is proportional to the capacitance according to the following relation:

$$I = 2\pi f V C \tag{2.2}$$

where f is the frequency of the excitation signal.

Figure 2.2 shows the simplified circuit to convert this current into voltage suitable for A/D converting. The actual capacitance of a tactile sensor unit is usually very small. Given a tactile cell with dimension $0.1in$ by $0.1in(2.54mm)$ and a $0.012in(0.3mm)$ silicone dielectric layer which has a dielectric constant $\epsilon_r = 5.0$, the effective capacitance is:

$$C = 8.85 \times 10^{-12} \times 5.0 \times \frac{(2.54 \times 10^{-3})^2}{0.3 \times 10^{-3}} = 0.95(pf) \tag{2.3}$$

It is not an easy job to precisely measure a capacitor this small using the above method because the parasitic capacitance and inductance introduced by sensor leads

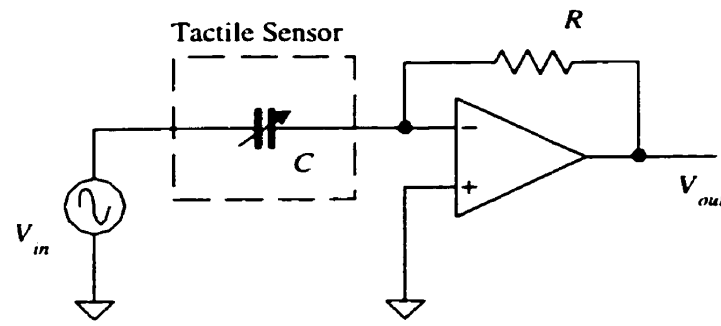

Figure 2.2: Basic tactile sensing unit

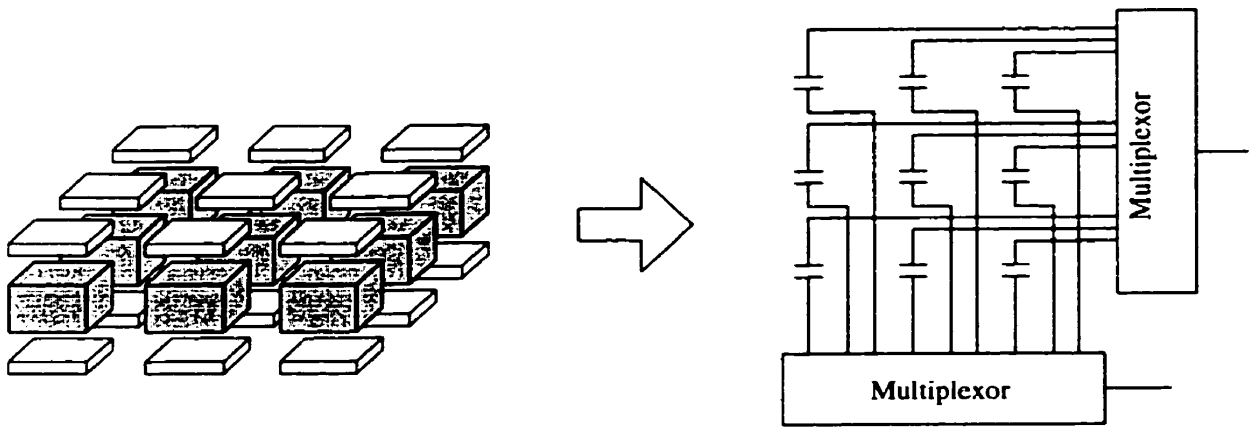

Figure 2.3: Complex multiplexing for a tactile array

and the measuring circuitry can contribute significant errors. Besides, the circuit shown above is a high gain, high impedance amplifier, a very small noise current coupled by the wire at the input will easily cause significant damage to the signal quality and integrity at the output. It is a big challenge for the implementation. There will be more discussion about this issue in the next chapter.

In order to stack a number of tactile sensors into an array, the multiplexing is needed. One method (Figure 2.3) is to construct each tactile cell individually and use independent multiplexing electronics for excitation and sampling.

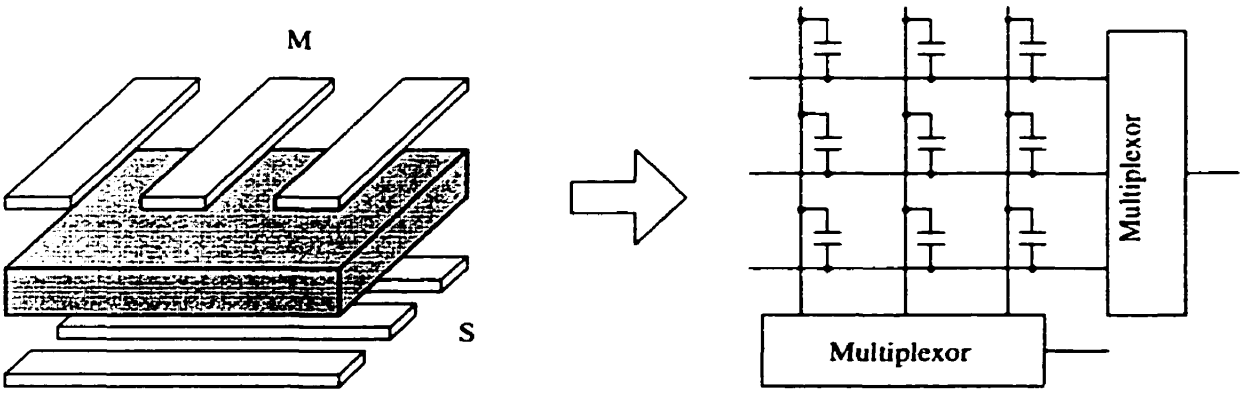

Figure 2.4: Built-in multiplexing for a tactile array

A better solution is to embed multiplexors into the architecture of the sensor array. Figure 2.4 illustrates this design concept. There are two sets of conductive strips, one functions as the static plates S and another functions as the moving plates M. A tactile cell is created at the intersection of each of $S(s)$ and $M(m)$ and is identified by (s, m) where s and m are indexes of the two conductive strip sets. The excitation and the sampling are conducted through $S(s)$ and $M(m)$. Compared to Figure 2.3, this method reduces the number of connections when there is a large number of tactile cells involved, thereby improves the reliability.

Chapter 3

Development

3.1 Design at System Level

The system architecture of the Intelligent Gripper System is directly based on its functionality defined in Section 2.1. As shown in Figure 3.1, there are three logical modules. They are the tactile subsystem, the proximity subsystem and the interface module. During the implementation, these three modules are not necessarily and exclusively at three physical localities.

To develop a good system level design strategy so as to achieve the best performance possible, we must first understand the physical restrictions and establish the design rules to deal with the real engineering problems caused by these restrictions.

3.1.1 Physical Restrictions and Design Rules

The most significant physical restriction for the implementation is the lack of space.

The Intelligent Gripper System is an electronic product prototype which is ready for production in small quantities. It is not a customized product where the high material and manufacturing cost can be tolerated. It also can not reach the quantity where the application specific technology such as Application Specific Integrated Circuits (ASIC) can be utilized. The only choice is to use off-the-shelf components and the mainstream

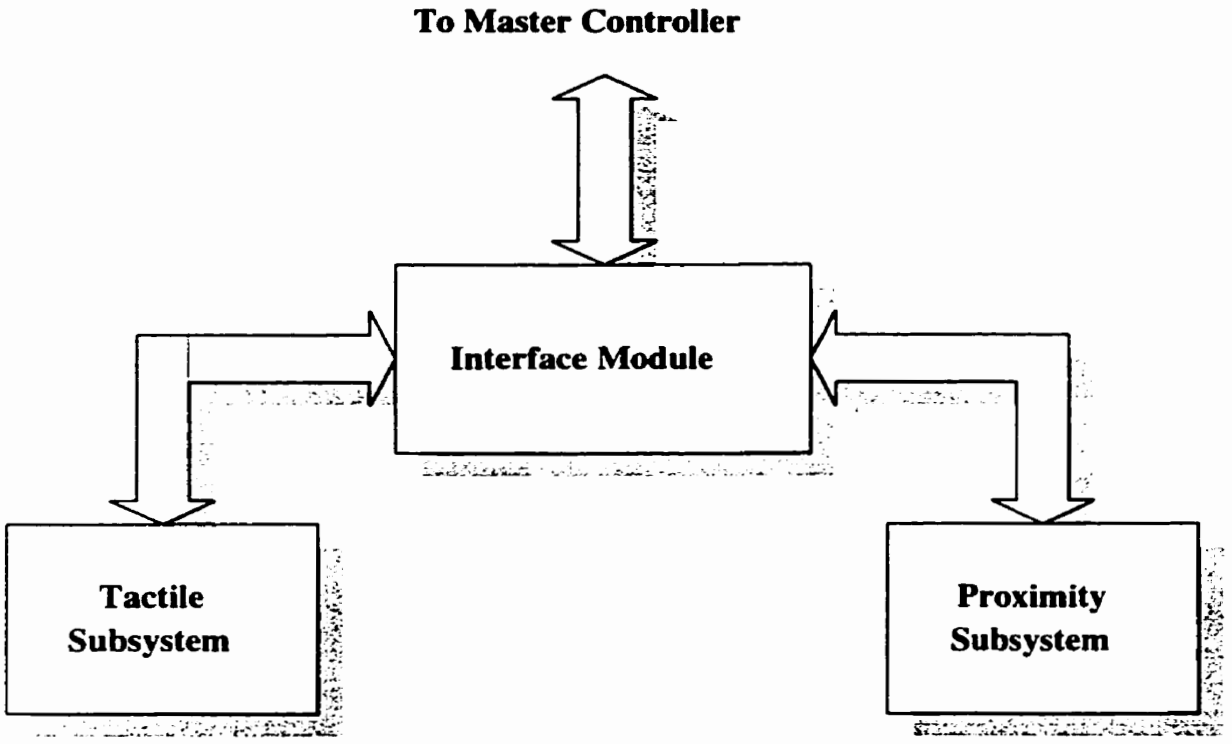

Figure 3.1: System level block diagram of the Intelligent Gripper System

manufacturing process.

Like any other human-sized robot arm, Sarcos Dextrous Slave Arm has a compact sized gripper. While the tactile sensor array and proximity sensor heads including LEDs and photo-transistors have to be located at the fingertip, there is barely enough room in or on the finger to house all the associated electronic components and protect them against wild movement of the gripper finger. The interface module, as defined in the last chapter, has the intelligent capability to exchange sensor readings and configuration information with master controller. Therefore it has to be a microprocessor or microcontrollor based device, if not implemented with complex logical circuits. In either case, it is more difficult to put the module at the same place where both sensors are located.

The solution is to pull some of the electronics away from the gripper finger and put them close to the wrist, or remove the electronics off the robot arm if necessary. This will certainly result in a modular design. It should be emphasized that, here a "module" is physical module, which does not have to match the logical modules exclusively(Figure 3.1). There could be less or more than three physical modules for the system.

While this sounds a good solution, it introduces problems and some could be serious.

First, the number of electrical connections among sensors, their associated electronics, the interface module and the master controller must be reduced to minimum in order to achieve good reliability. Meanwhile, all the wires have to be kept as short as possible. This requires careful planning.

The second problem might be more significant. The Intelligent Gripper System is a mixed analog/digital system. An improper inter-module wiring will cause severe defect to the quality and integrity of small signals, in particular, the raw signals from tactile sensors and photo-transistors. There are four types of electrical signals involved.

1. The small analog signals generated from both sensors and transferred to their associated electronics for preliminary processing.

2. The large magnitude analog signals transferred from sensor electronics to analog-digital converting device.

3. The TTL level digital signals mainly presented in the interface module and the master controller.

4. The power rail along with the ground connecting all components.

The broad band Radio Frequency (RF) noise may be the most common source of noise to high gain, high impedance amplifiers which are used in both tactile and proximity sensing subsystems. RF noises are normally generated by the brush of DC motors and Pulse Width Modulation(PWM) power supplies, both are heavily used in a robotics laboratory environment. An unshielded floating wire can easily pick up RF interferences strong enough to cause an electrical system to malfunction. Since this type of noise has a very broad spectrum, it is very difficult to apply filtering without significant delay.

Besides RF interference, the sharing of the power supply and the common ground by digital and analog components introduces additional noise, typically the ground bounce or power dropping caused by Simultaneous Switching Operation (SSO) of digital devices. The digital devices also consume much more power than analog components and generate much stronger high frequency disturbances on the power rail and ground.

Based on these arguments, a set of design rules has been identified. To achieve the expected system performance, these rules have to be strictly enforced.

1. The system is composed with a number of physical modules. Keep analog circuitry and digital circuitry away from each other in separate physical modules. There should be no small analog signals transmitted between physical modules. The occurrence of mixed analog and digital signals exchange between any two modules must be kept to the minimum or eliminated.

2. The tactile sensor array and its pre-processing circuitry must be kept as close to each other as possible. A single compact physical module with good shielding is strongly recommended. The same principle and requirement applies to proximity sensors as well. However, due to the limited space at the gripper finger tip, it may not be possible to fulfill this requirement for both sensors. The tactile sensor has a higher priority.

3. The analog circuitry must not share power supplies with the digital circuitry. In the analog circuitry, the small signal part should be at the far end of the power rail and a decoupling network must be used. While the entire system may have to share a common ground, effective noise de-coupling measures must be applied.

4. An optimized system architecture should be developed to reduce the number of inter-module connections to the minimum. This will make the system more reliable and will improve its portability.

3.1.2 System Architecture

Following the design specification and rules, the overall modular architecture is established as shown in figure 3.2.

Similar to functioning modularity, there are three physical modules. The tactile sensing module, the proximity sensing module, and the interface module.

The tactile sensing module includes a tactile sensor array and its associated electronics. The task of the electronics is to preprocess the raw tactile information, to multiplex and to de-multiplex. All the relevant small signal processing is constrained in this module. The entire module is a solid state device constructed from a base Printed Circuit Board(PCB) and there is no out-of-PCB wiring.

The proximity sensing module is very similar to the tactile sensing module. However, due to the limited space on the finger tip, there are soft wirings between sensor

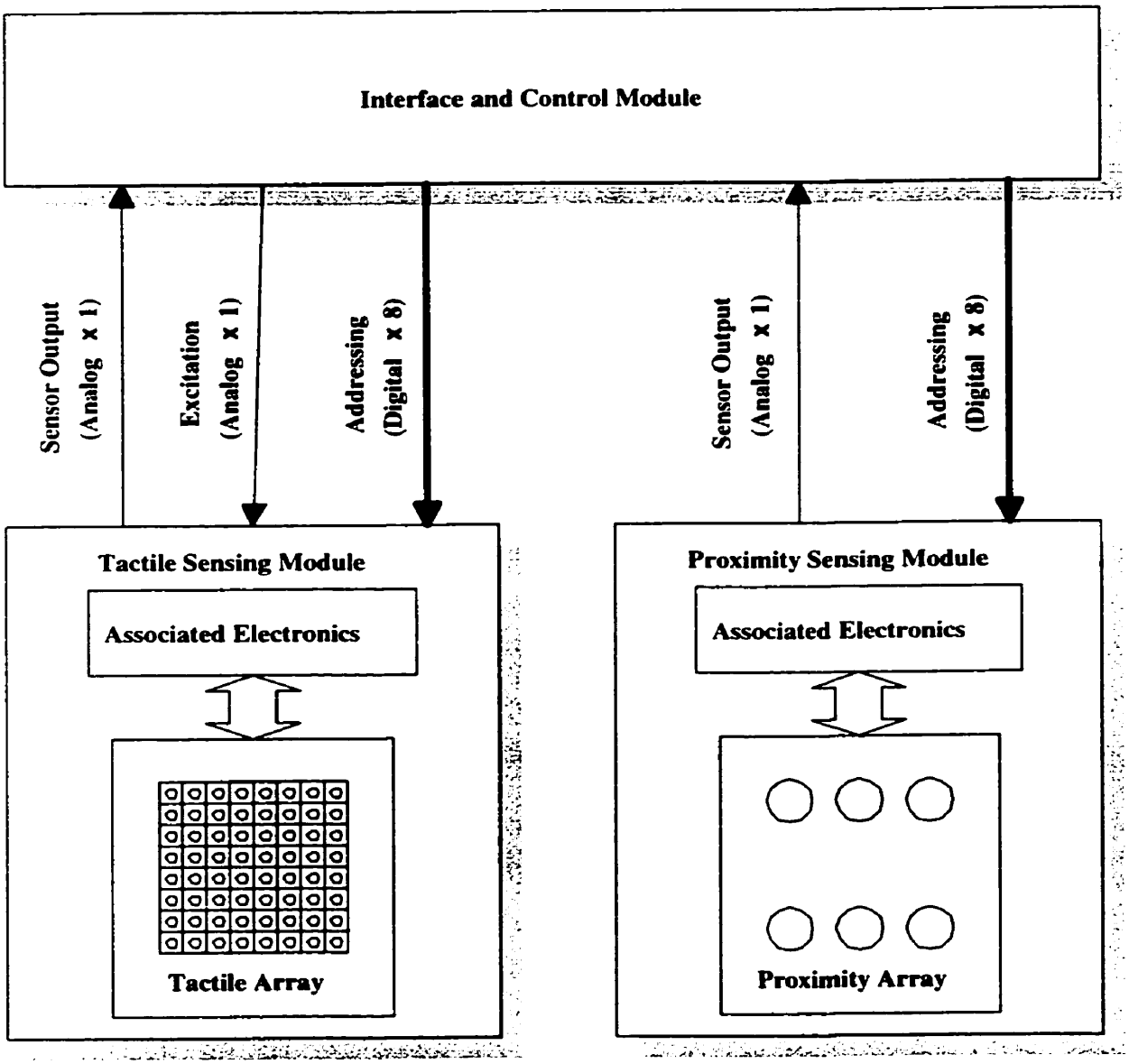

Figure 3.2: Modular architecture for the Intelligent Gripper System

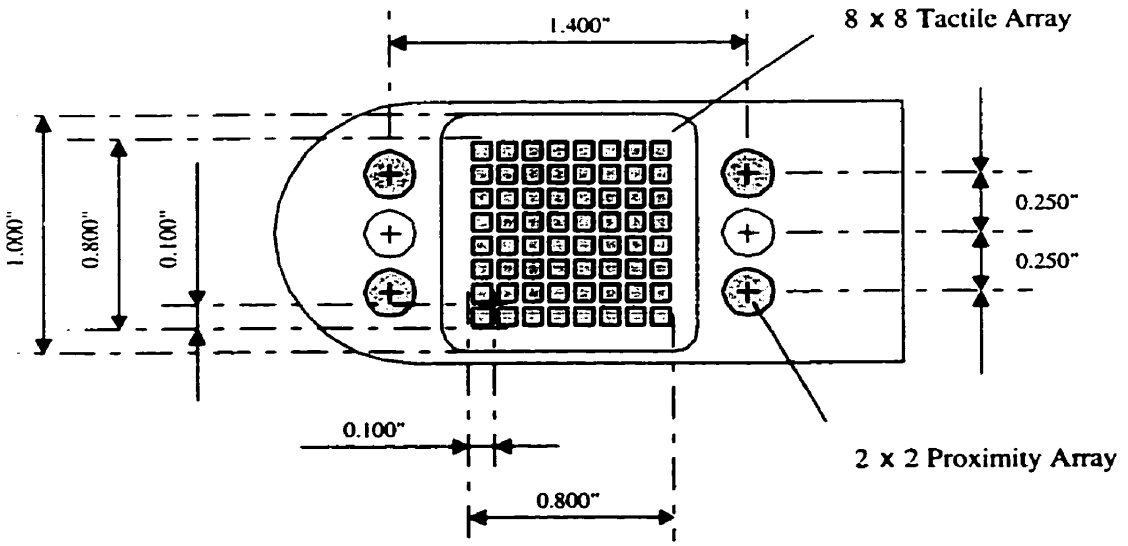

Figure 3.3: Layout of the gripper finger

heads and the circuitry. All the relevant small signal processing and multiplexing/de-multiplexing are restrained in this module.

The interface module has the functionality defined in Chapter 2. It conducts the control and the configuration to two sensing subsystems and converts sensing signals from analog waveforms into digital data. Besides, this module has a part of the analog circuitry for the tactile sensing subsystem. This part of the circuitry is mainly pre-A/D converting processing, like gain and offset scheduling.

The analog and digital signals transmitted between three modules are also shown in figure 3.2.

Figure 3.3 is the physical layout of the gripper finger. In the center is a 8×8 tactile sensing array. The four channel proximity sensors are located at the four corners of the finger. Instead of using one LED in each proximity sensor head, each LED is shared by a pair of photo-transistors and is located in the middle of them. This configuration saves the space and simplifies the circuits.

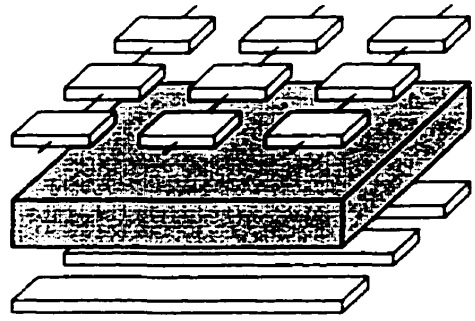

Figure 3.4: Modified tactile array with built-in multiplexing

3.2 Tactile Sensing Subsystem

3.2.1 Tactile Sensing Array

In Chapter 2 the principle of the capacitive tactile sensing has been explored. Figure 2.4 shows the simple strip structure of the tactile array. However, from the experiment and the application practice, it is found that this construction has a few problems.

First, the top conductive strip introduces "soft" electrical connections between its floating base and other PCB based components, and therefore makes it very difficult to simplify the fabrication process. This configuration is not very suitable for solid state design. Second, the rigidity of the top conductive strip will possibly cause mechanical coupling between adjacent sensor cells, and therefore reduces the spatial resolution of the sensor. Under high load, the top strip may be permanently bent which results in a dramatic change of sensor characteristics. One approach to solve this problem is to change the top strip into conductive pads connected by thinner strips as shown in Figure 3.4. But if the strips are too thin, they are more likely to be broken when the sensor is under large load.

Figure 3.5 shows a much more robust construction developed by David Johnston [JZH96] of Sarcos Research Inc. (390 Wakara Way, Salt Lake City, UT84108).

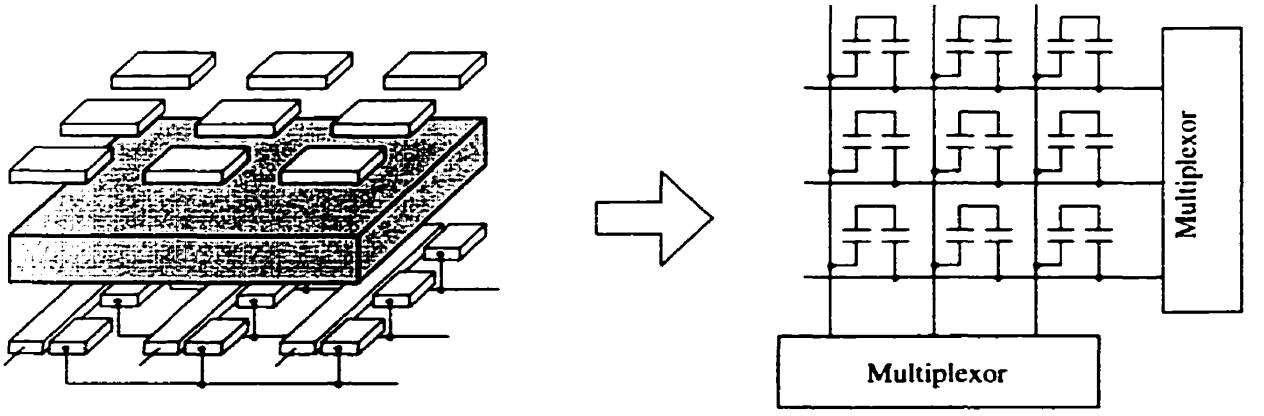

Figure 3.5: Dual strip with floating plate tactile array

Instead of using the electronically connective strips, a dual static bottom strip with a floating conductive plate configuration is utilized. The shortfall of this design is that it changes the original sensing capacitor into a couple of sequentially connected capacitors of half capacitance. The resulting sensor capacitance is at least 75 percent smaller.

Shown in Figure 3.6, the tactile sensor subsystem is constructed on a printed circuit board, the back board. On one side of the back board, the sensor array is constructed and on the other side another PCB for the associated circuitry is attached.

The dual static strip of the tactile sensor is implemented by the copper foil of the back board through a proper PCB layout. The floating plate is implemented by the PCB technology applied on kapton. Kapton is a film like flexible PCB with a 2 to $5mils$ (a thousandth of an inch) thick base. To reduce the spatial crossing of the tactile sensing array, the thinnest kapton available is used. It has a 2-mil base and a 1 mil copper foil. Figure 3.7 shows the physical dimension of the static strip, the floating plate in a single cell.

The dielectrical layer is implemented with R-2186 silicone rubber from Nusil Silicone Technology Inc. (1050 Cindy Lane, Carpinteria, CA93013).

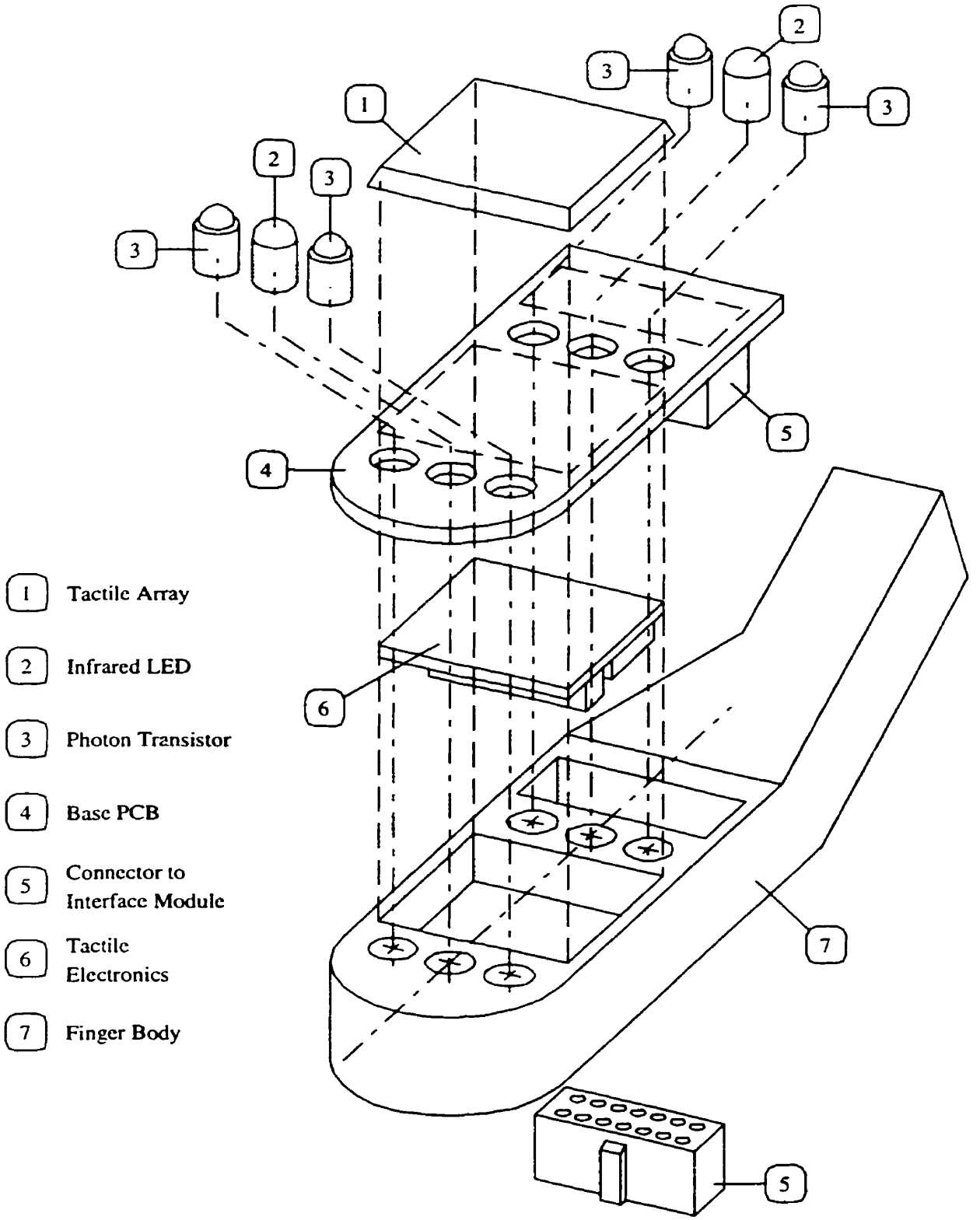

Figure 3.6: Assembly of gripper finger with tactile and proximity sensors

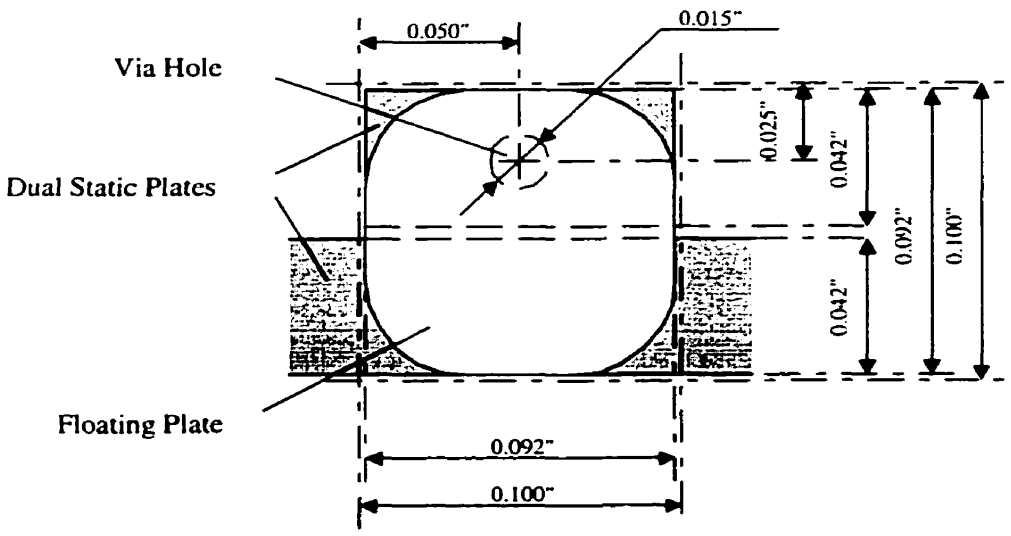

Figure 3.7: Physical dimension of a tactile cell

Above the floating plate layer and the kapton, there is an additional layer for protection and Electrical-Magnetic (EM) shielding. As discussed earlier, the tactile sensor electrodes, the two static strips, are directly connected to a high impedance amplifier. The tiny noise picked up by them will cause significant damage to the signal-noise ratio. Theoretically, it is necessary to cover the entire sensor with conductive and well grounded material. One type of this shielding material is R-2637, also from Nusil. However, experiment shows there are shortfalls brought by the shielding layer and more in-depth analysis will be presented in chapter 5.

3.2.2 Tactile Sensing Electronics

Figure 3.8 is the block diagram of the supporting circuits of the tactile array.

Each sensor cell has two connections, one for the excitation input and the other for the sensor output. The system works in the serial manner in which only one sensor is excited and sampled at one time. Therefore multiplexors are implemented for both the excitation and the sensor output. The device used is the CMOS one-to-eight analog

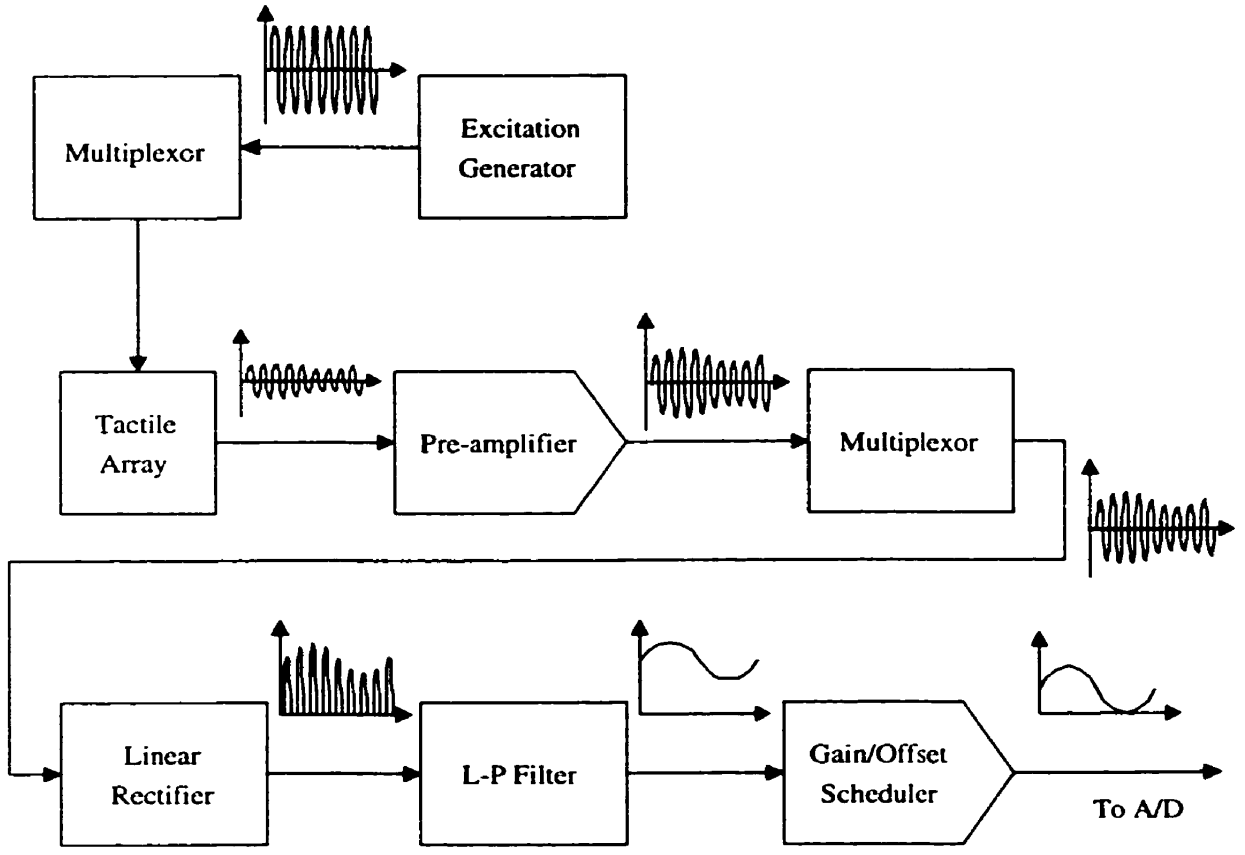

Figure 3.8: Block diagram of tactile array supporting circuitry

switch 74HC4051. It has a low switching resistance of 50 Ω.

There is a pre-amplifier associated to each row (eight in total) before the raw sensing signals are multiplexed. The reason not to multiplex the raw current signal is because its magnitude is very small while the multiplexor which behaves as a switch generates huge wide band noise. The signal-noise ratio will be catastrophically damaged if the multiplexing is immediately applied to the sensor. The pre-amplifier acts as a buffer. It converts the raw sensing current into relatively large voltage which is much easier to handle.

Referring to Figure B.2, the multiplexed sensor output is forwarded to the linear rectifier (U06C) where the AC voltage is converted to a DC signal, followed by a low-pass filter (U06A). Before it is forwarded to the A/D converter, the signal goes through the offset scheduling circuit.

The tactile sensor response can be represented by this simplified model:

$$V_s = ax + b \tag{3.1}$$

where V_s is the sensor response and x is the stimuli.

While the capacitance based tactile sensor output has a large offset b representing the static (idle) capacitance, only the change of this capacitance is useful. If the signal is directly sent to the A/D converter, a large part of the A/D resolution will be wasted. This is especially true when the dynamic range of the sensor output is relatively small compared to the offset. To solve the problem, an offset scheduling scheme is implemented as shown in Figure 3.9.

The output of D/A converter D/A(1) along with the raw sensor output are sent to a subtracter (U06D) which outputs

$$V_0 = -\frac{R_{010}}{R_{09}}V_s - \frac{R_{010}}{R_{013}}V_f \tag{3.2}$$

The microprocessor sends the calibrated offset value V_f of the individual sensor cell through D/A(1). Combining 3.1, 3.2 becomes

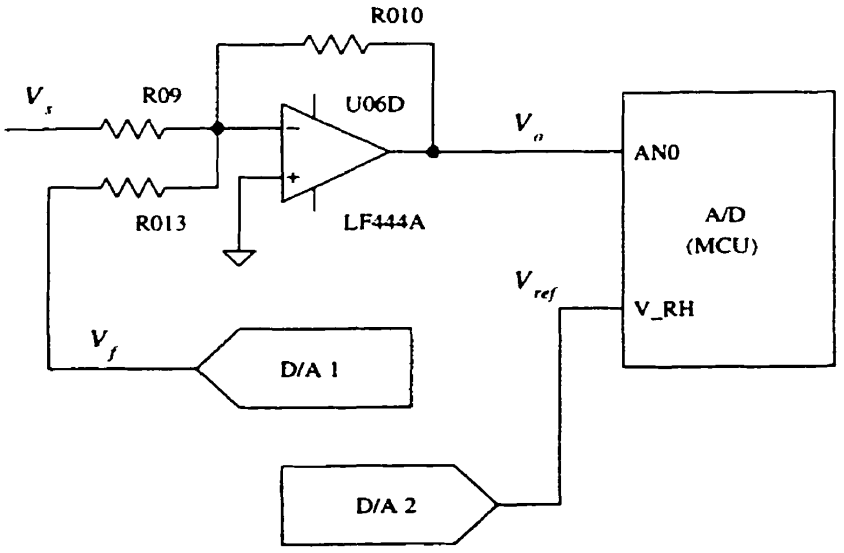

Figure 3.9: Offset and gain scheduling for tactile sensing

$$V_0 = -\frac{R_{010}}{R_{09}}ax - \frac{R_{010}}{R_{09}}b - \frac{R_{010}}{R_{013}}V_f \tag{3.3}$$

choose

$$V_f = -\frac{R_{013}}{R_{09}}b \tag{3.4}$$

We have

$$V_0 = -\frac{R_{010}}{R_{09}}ax \tag{3.5}$$

As a result, the offset is eliminated.

The maximum magnitude of individual sensor outputs may be diversified dramatically. In order to utilize the full scale of the A/D converter, sensor outputs have to be normalized. Illustrated in Figure 3.9, a gain scheduler is implemented. Through D/A(2), another D/A converter, the microprocessor sets the reference voltage of the A/D converter at the level of maximum output of the tactile cell being sampled:

$$V_{ref} = -\frac{R_{010}}{R_{09}} a x_{max} \tag{3.6}$$

The A/D reading is

$$V = \frac{V_0}{V_{ref}} = \frac{x}{x_{max}} \tag{3.7}$$

The A/D reading is normalized.

The $100KHz$ sinusoid excitation signal is generated by XR-2206, a universal signal generator. According to Equation (2.2), the magnitude of the sensor output is proportional to the excitation frequency. However, it can not be too high due to the limited bandwidth of the amplifier. The device used is an LF444 low noise OP amplifier whose cut-off frequency is $2MHz$. $100KHz$ is the trade-off frequency for optimized performance.

Since there is only limited space on the gripper finger, only the sensor array, the multiplexors and the pre-amplifiers are located on it. While the tactile sensor array is at the contacting surface of the finger, all the other components are located on a small PCB which is attached on the back of the base PCB and embedded in the body of the finger. This structure not only gives greater physical protection but more importantly, shields the small signal electronics against electrical and magnetic contamination.

3.3 Proximity Sensing Subsystem

Figure 3.10 shows the block diagram of the circuitry supporting a 2×2 infrared LED-photon-transistor proximity sensing array. Essentially, the entire signal processing is similar to that of the tactile subsystem.

Each proximity channel has its own pre-amplifier in order to reduce switching noises caused by the multiplexor. In contrast to the tactile excitation, the LED is driven independently and each LED is shared by a pair of sensing devices. This configuration simplifies the design by utilizing the active nature of this type of sensing devices. The

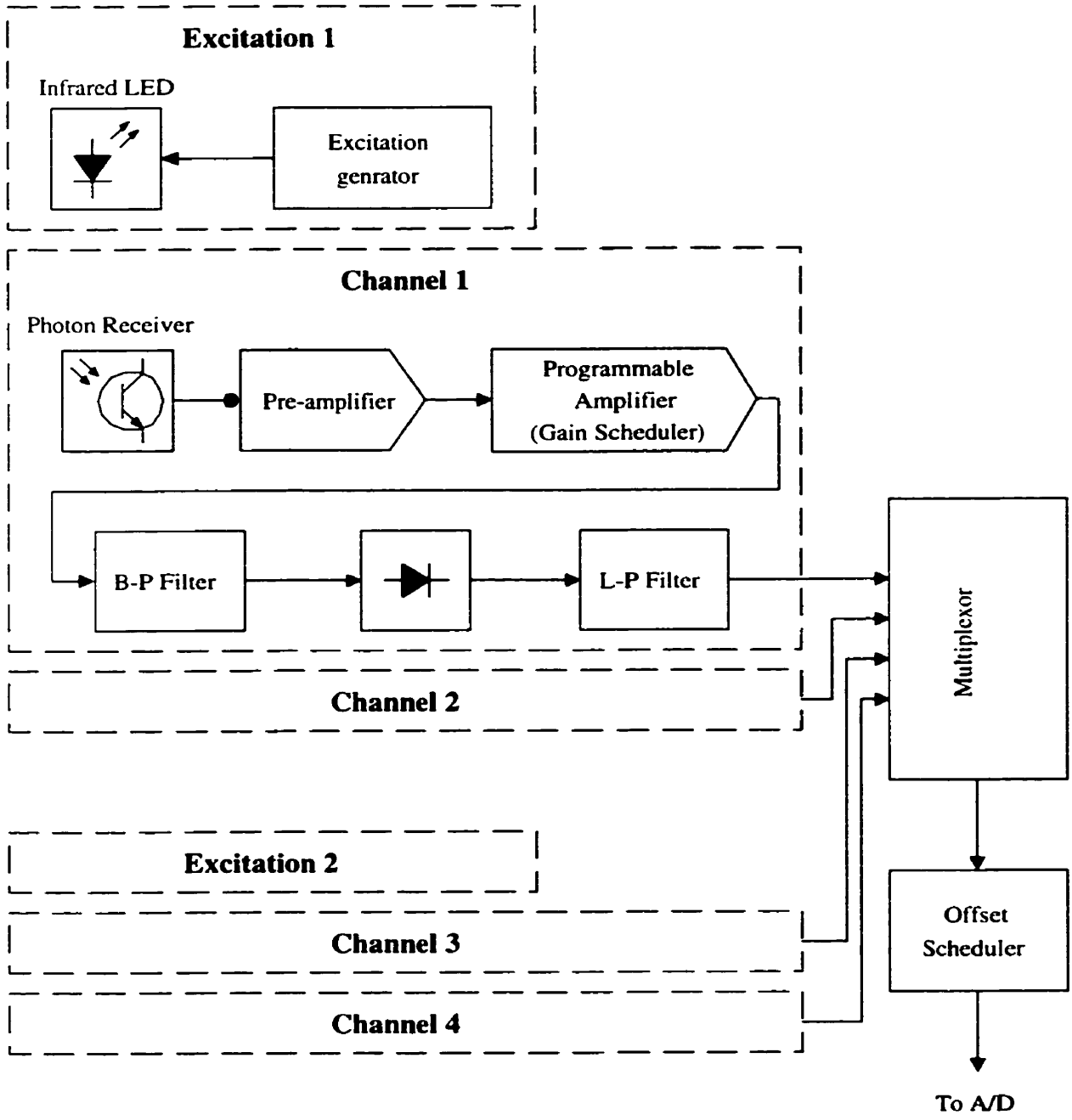

Figure 3.10: Block diagram for proximity sensing array (four channels)

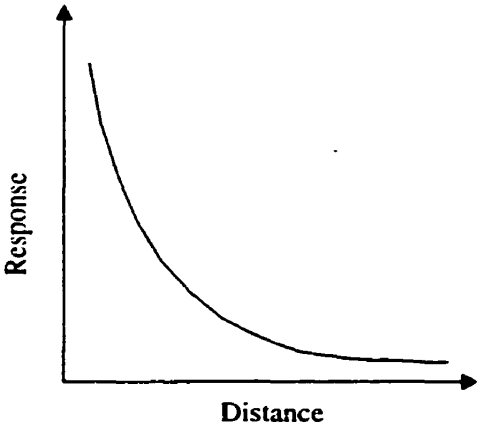

Figure 3.11: Typical response of a infrared LED/photon transistor proximity sensor

system uses the same device for the multiplexing and the excitation signal generating as that used in the tactile subsystem.

While an offset scheduling mechanism same as that of the tactile is implemented, the gain scheduling is different. According to Petryk and Buehler [PB96], the response of the proximity sensor is extremely nonlinear over the sensing range as shown in Figure 3.11.

In order to utilize the full scale of the A/D converter, not only different channels must be balanced, but also the response curve of the individual channel has to be segmented and sampled separately. To fulfill this requirement, a programmable amplifier is implemented (Figure 3.12).

By selectively and turning on K_1 and/or K_2, the gain is changed based on (3.8).

$$G = 1 + \frac{R_{08}}{R*} \tag{3.8}$$

where $R*$ is determined by the combination of R05 ($1.0M\Omega$), R06 ($47K\Omega$) and R07 (68Ω).

K_1 and K_2 are implemented by analog switch 74HC4051, the same device used for multiplexing. The actual value of $R*$ and the corresponding gain is listed in Table 3.1.

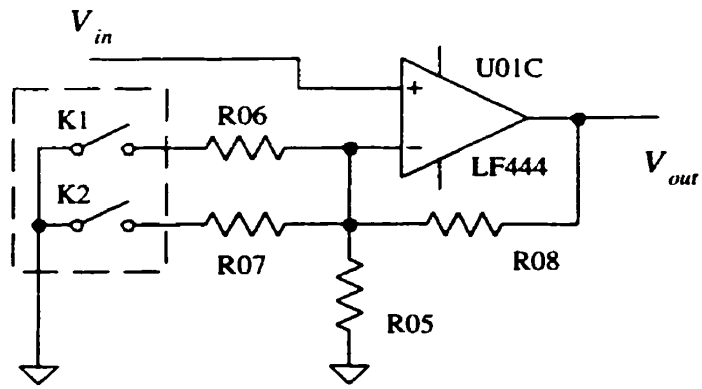

Figure 3.12: Programmable amplifier for proximity sensing to eliminate saturation and to increase the sample resolution

K_1	K_2	Gain
off	off	1.00
off	on	7.33
on	off	1.01
on	on	7.34

Table 3.1: Available gains of the programmable amplifier

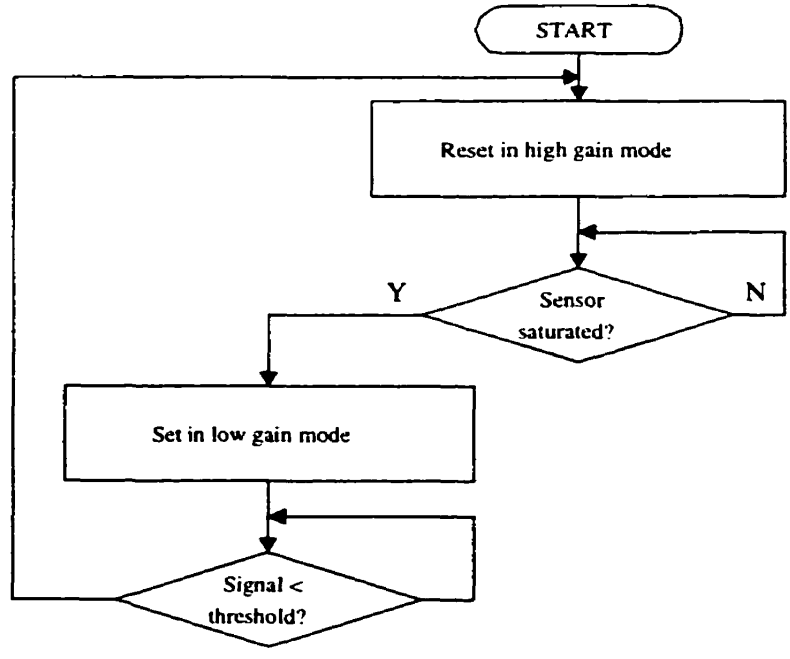

Figure 3.13: Flow chart for gain scheduling mechanism

When the proximity sensor is working on a large sensing range, the high gain switch K_1 is turned on. In the case the object is close to the gripper, K_2 is turned on.

Because the sensor has no priori knowledge where the object is, it is not able to determine whether it should operate in the high gain or the low gain mode at the first place. A thresholding mechanism is designed to facilitate the decision making. Initially, the sensor is set in the high gain mode, if a saturation in the output is observed, it turns into the low gain mode immediately and stays in this mode until the output level is under a predefined threshold. In this case the sensor switches back to the high gain mode and keeps monitoring the output until the saturation occurs. Figure 3.13 shows the flow chart of this process. It is run by the microprocessor on the interface module. The threshold in the current design is 0x20 on A/D reading representing 12.5 percent of the full 8 bit A/D scale.

3.4 Interface Module

3.4.1 Architecture

Logically, the interface module is the "brain" of the entire Intelligent Gripper System. It coordinates the operation of both sensor subsystems and regulates the data flow between them and the master controller.

Figure 3.14 shows the functional block diagram. The central part is MC68HC11E2, an eight-bit micro-controller (MCU). All the other components are essentially peripheral devices connected to it through the data bus, the address bus, and the control signals.

The MC68HC11E2 has an internal 2KB EEPROM (Electrical Erasable Programmable Read Only Memory) and a 256-byte RAM bay. These memory resources are adequate to implement the application software through proper coding. Currently, there is no external ROM and RAM installed. The MC68HC11E2 has four operational modes selected by MODA and MODB pins. They are listed in Figure 3.20. Two modes may be activated in the current design. The special boot strap mode is only for EEPROM programming and/or updating. Under the normal situation, the micro-controller is operating in normal extended mode in which more external peripheral devices can be supported.

P_t is an eight-bit unidirectional output parallel port which is used to latch the multiplexor input commands issued by MCU to the tactile sensing subsystem. Any of the sensor cells in the array can be addressed (excited and sampled) by writing the proper octet to P_t. Figure 3.15 shows the mapping between the address and actual cells.

P_p serves the similar role as P_t does for the four-channel proximity sensing subsystem. In addition to sensor addressing, the gain scheduler is also controlled by MCU through P_p.

Both P_t and P_p are implemented by 74HC374, U010 and U011 respectively, as shown

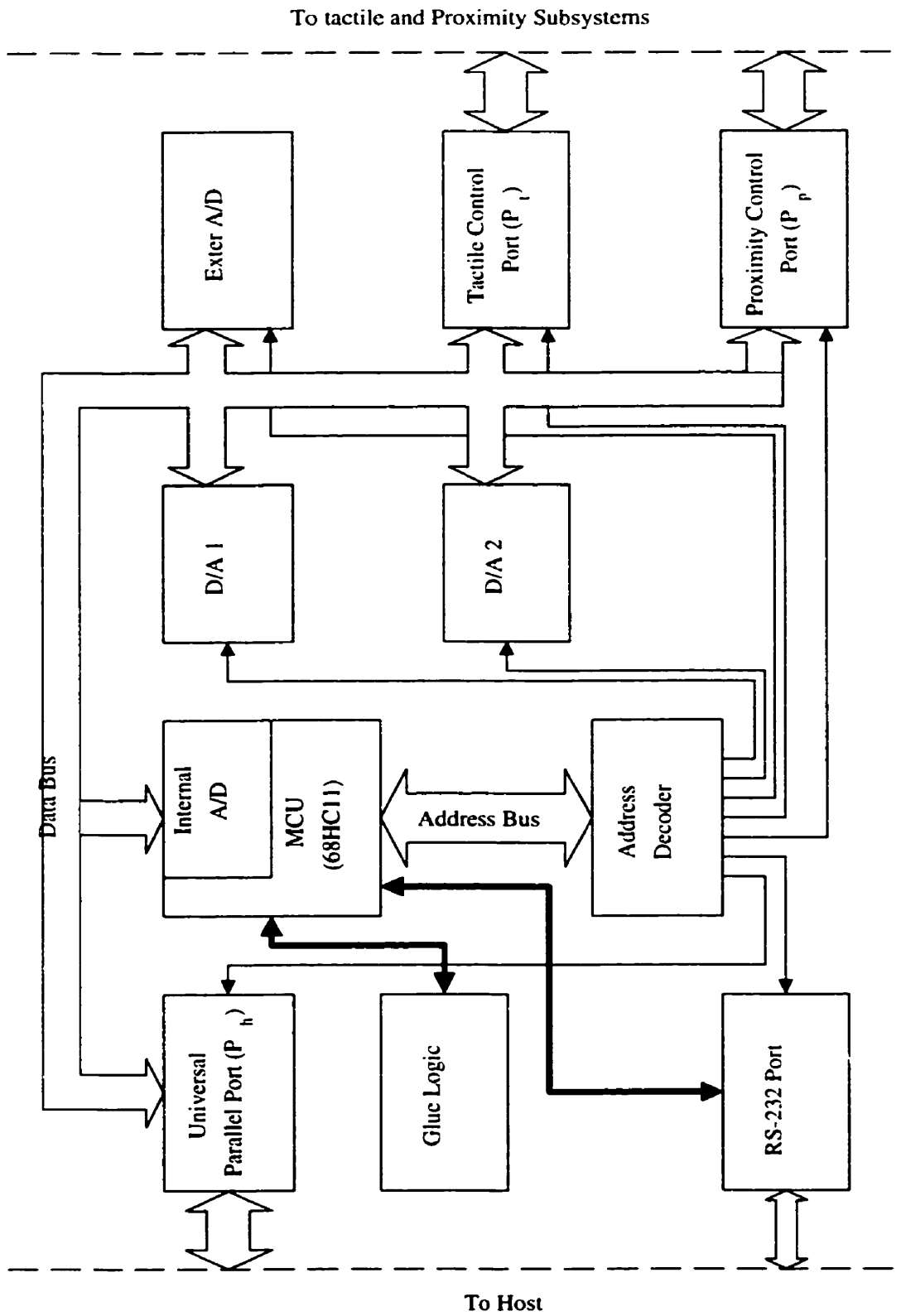

Figure 3.14: Block diagram of interface module

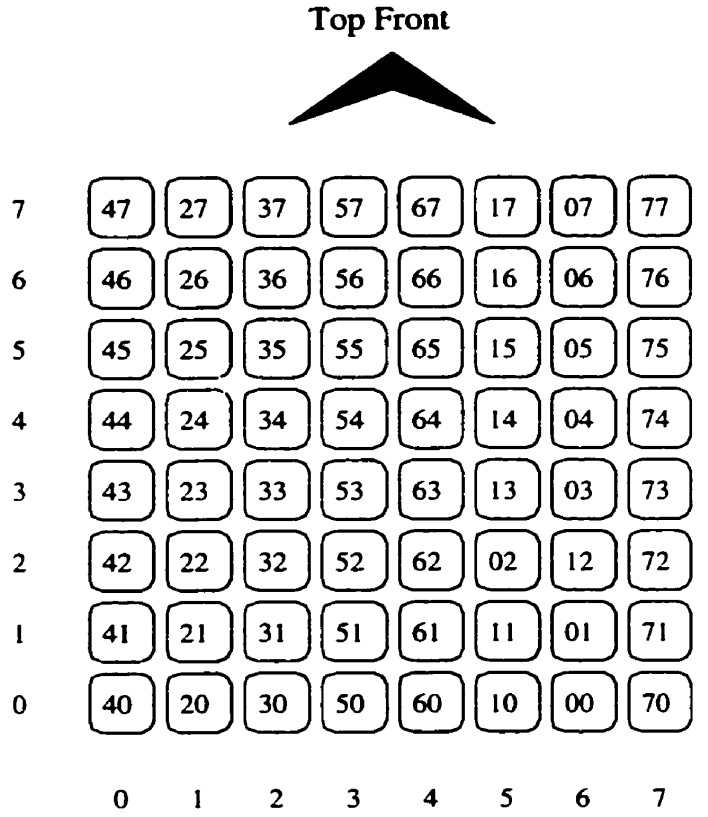

Figure 3.15: Tactile cell address mapping (top view)

Signal Name	Pin Number	Direction
OSTR	1	Input
GND	2 to 6	NA
MODB	7	Input (Set to high/low internally)
MODA	8	Input (Set to high/low internally)
RESET	9	Input (Set to high internally)
IHS	10	Input
OHS	11	Output
ISTR	12	Output
DB(8)	13 to 20	I/O

Table 3.2: List of signals of host interface P_m

in Figure B.2

P_m is a universal parallel port used to communicate with the master controller. It has an eight bit bi-directional data bus and five control signals for hand-shaking. While the data bus is implemented with 74HC244 and 74HC374 (U021 and U020 in Figure B.3), the control signals use general purpose I/O lines of the MCU and they can be configured either as input or as output. Figure B.3 shows the schematics of P_m and Table 3.2 lists the names and directions of the control signals. Notice MODA, MODB and RESET are only used by the master controller for reset and initialization. Figure 3.16 gives the bus/hand-shaking cycles for P_m read and write operations.

D/A(1) (U07) and D/A(2) (U08) are eight bit digital to analog converters AD558. They are used for gain and offset scheduling for both sensing subsystems, as described earlier. These devices are UP compatible, therefore no additional component is needed to interface with MCU (Figure 3.17).

According to the design functionality and specifications, the interface module must send sensor readings to the master controller only in the digital format. Therefore, all the analog signals from sensors must be digitized in the interface module. Fortunately, 68HC11 comes with an internal 8-bit A/D converter. It has the minimum converting time of $20\mu s$. Considering the sub one hundred bandwidth of a typical robot system,

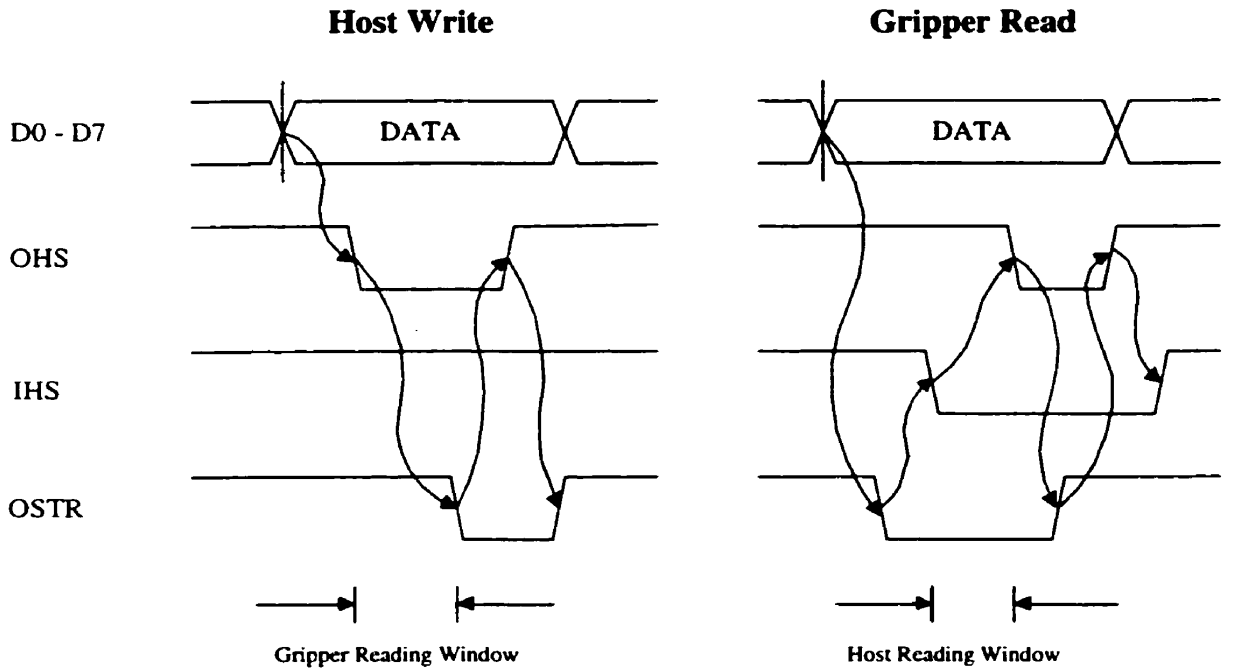

Figure 3.16: Read/Write cycles of the parallel port

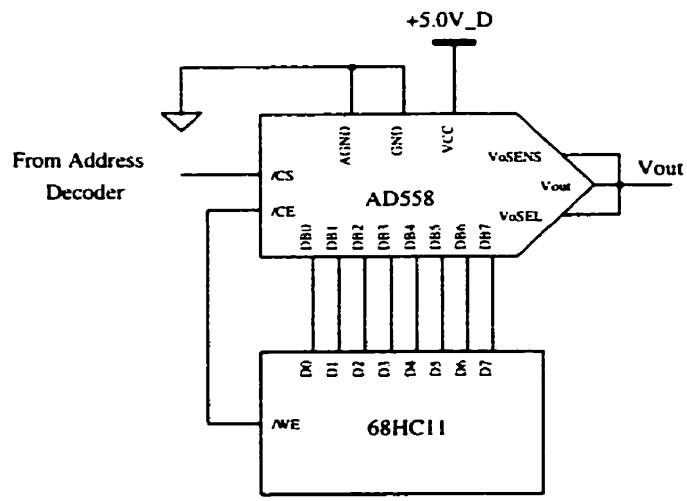

Figure 3.17: Interface between AD558 and MCU

it is adequate to serve this purpose. An external 14-bit UP compatible A/D converter AD7871 (U09) is also employed (Figure 3.18) in case eight bit resolution is not high enough for analysis.

MC68HC11 has its internal serial communication port (SCI) complying with the RS232 format. While this port can be activated by the application for data collecting/transmitting, it serves a more critical role to let users download programs into EEPROM. A voltage translator MAX202 is employed to translate MC68HC11's TTL level to RS232 level and vice versa.

The only address space available for 68HC11 is the memory space. All the parallel ports, D/A devices and external A/D devices are mapped into this space through the address decoder (U02 in Figure B.1). Table 3.3 lists the addresses of all external devices. The access to the internal A/D and serial port is through dedicated instructions. Therefore, they are not mapped in this space.

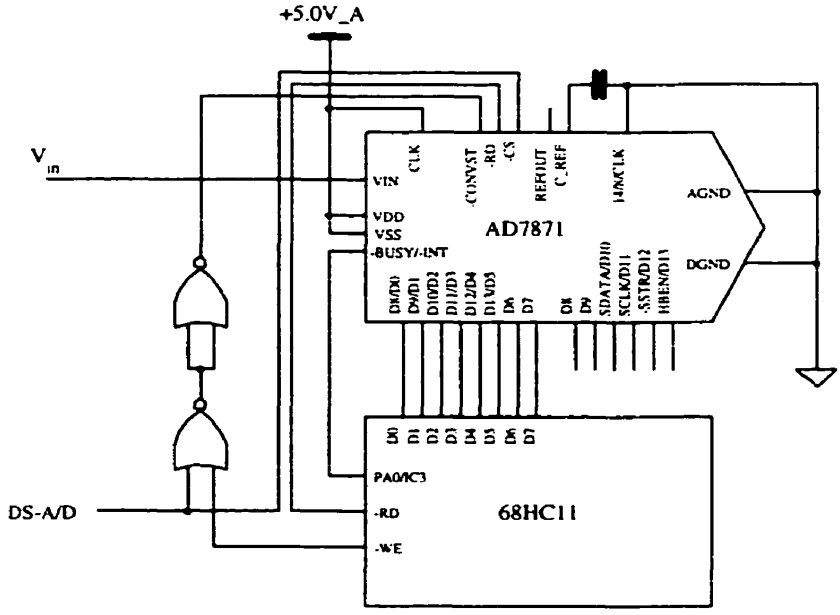

Figure 3.18: Interface between AD7871 and MCU

Address	Device
0xEE00	Reserve
0xEE01	Proximity control port P_p
0xEE02	D/A(1) for offset scheduling
0xEE03	Host port P_m
0xEE04	D/A(2) for gain scheduling
0xEE05	Tactile control port P_t
0xEE06	14-bit External A/D
0xEE07	Reserve

Table 3.3: Address of external devices

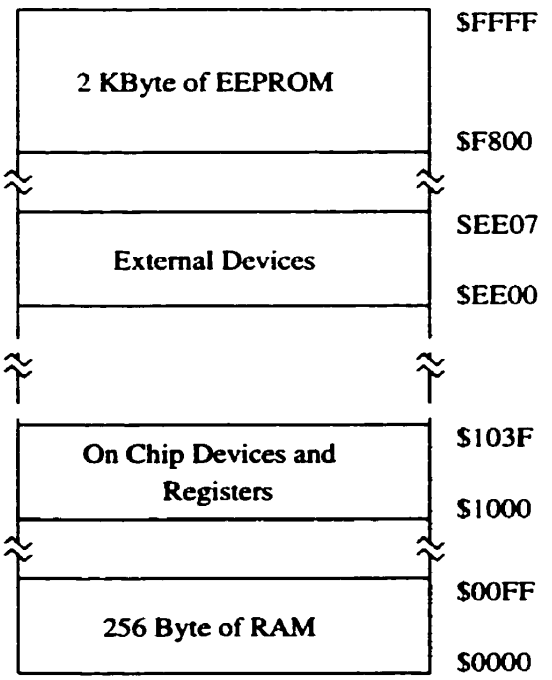

Figure 3.19: System hardware resource mapping

3.4.2 Boot Strap and EEPROM Programming

The only way to download the application software into the EEPROM of the MC68HC11 for the first time or reload the revision is through its internal serial port, after the MCU has been reset in the special boot strap mode, which is determined by MODA and MODB pins. Figure 3.19 and Figure 3.20 are the MCU resource mapping and the mode selection with the corresponding reset vector.

When the MCU is reset in the special bootstrap mode, a small on-chip ROM is enabled at address BF40-BFFF. The reset vector is fetched from this bootstrap ROM. The program in this ROM initializes the on-chip SCI interface, checks security option, accepts a 256-byte program through the SCI, then starts to execute the loaded program at address 0x0000 in the on-chip RAM. There is almost no limitation on the programs that can be loaded and executed through the bootstrap process.

The Loader, a 256-byte program downloaded through SCI and executed immediately

Inputs		Mode Description	Reset Vector
MODB	MODA		
1	0	Normal Single Chip	$FFFE, FFFF
1	1	Normal Expanded	$FFFE, FFFF
0	0	Special Bootstrap	$BFFE, BFFF
0	1	Special Test	$BFFE, BFFF

Figure 3.20: MCU mode selection with the corresponding reset vector

afterwards is developed. It reinitializes SCI and accepts the application programs and burns the code into on-chip EEPROM byte by byte. Figure 3.21 shows the block diagram of the Loader. The instructions are listed in Appendix C.

To facilitate the development, an Intelligent Gripper Diagnostic System (IGDS) is also developed. It has a graphic user interface and runs in the PC-Windows environment. The IGDS uses RS-232 serial port to communicate with the gripper system. It not only has utilities for application program downloading and debugging, but also collects all the sensor readings and displays them graphically. The IGDS greatly reduces the complexity of the development and the debugging procedure of this embedded system.

3.4.3 Drivers

The EEPROM residing program is written in Motorola assembly language and is hierarchically organized.

On the top there are three principal tasks. They are the application task, the demo task and the testing task. The application task performs all the real time application routines of the Intelligent Gripper System. The demo task works with IGDS to display tactile and proximity images in the IGDS environment. The testing task also runs with IGDS to test and debug the Intelligent Gripper System. While the only parallel port P_m is occupied by the application task only, the other two tasks use the serial port to

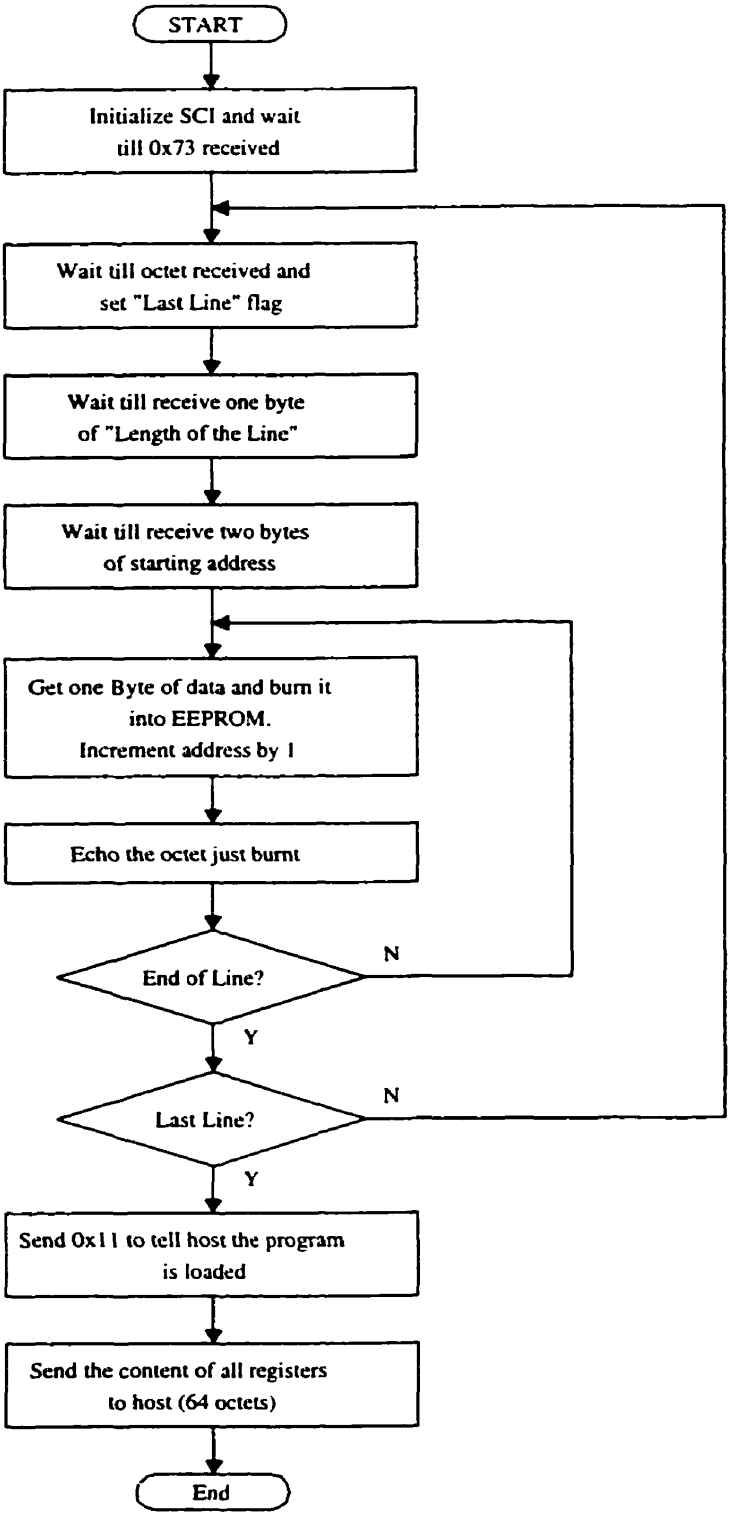

Figure 3.21: Block diagram of Loader

exchange sensor readings and control parameters with IGDS.

By default, the system starts the application task after the reset. It is branched into the demo task or the testing task at any time after the MCU receives branch command octet (0x80 in demo task, 0x40 in testing task) through SCI. The program always returns to the application task as soon as MCU receives termination command octet (0x81 in demo task, 0x41 in testing task).

Figure 3.22 shows the top level block diagram. Figure 3.23, Figure 3.24 and Figure 3.25 are block diagrams of the internal structure and organization of the three principal tasks. The list of assembly code can be found in Appendix C.

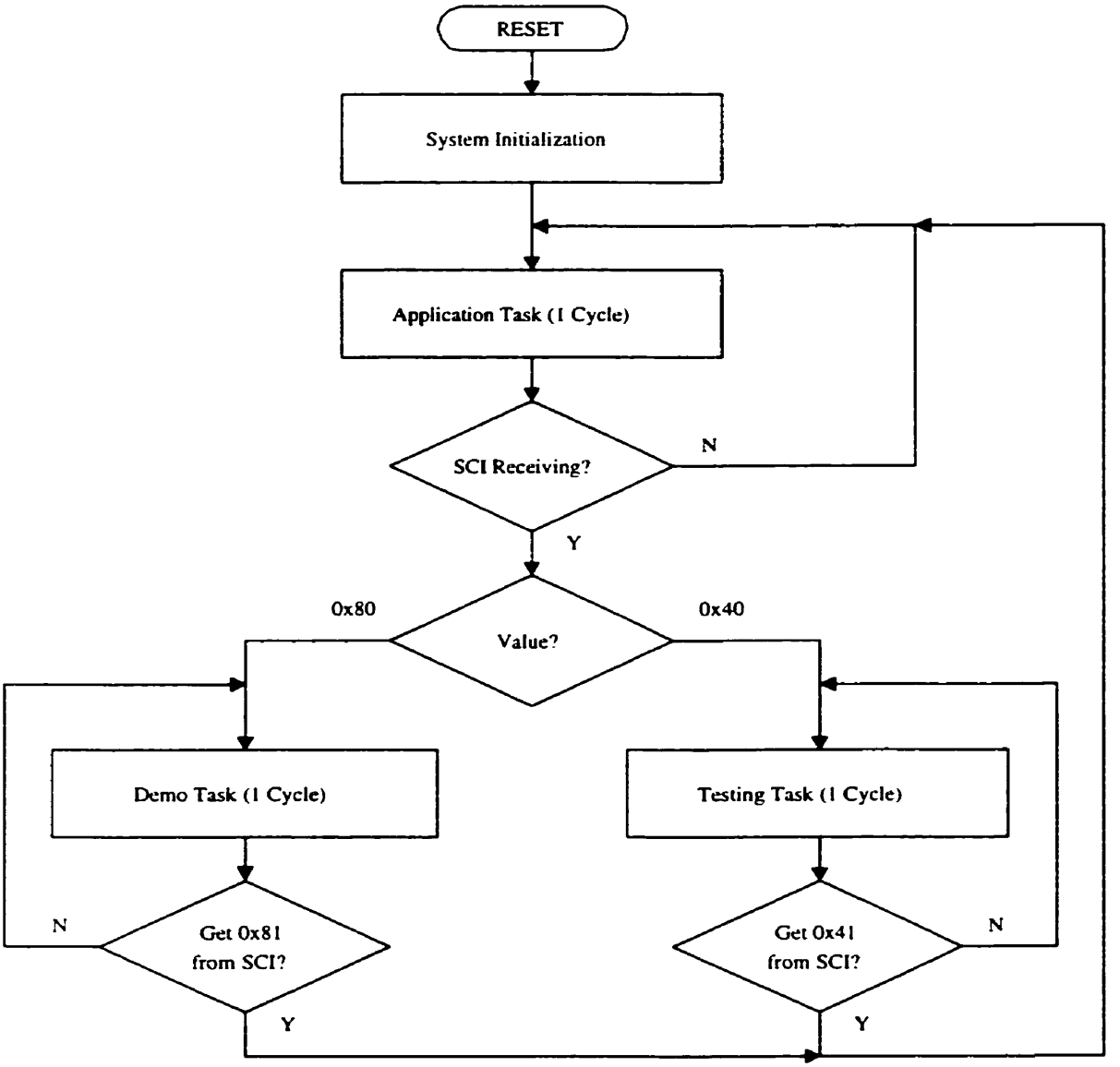

Figure 3.22: Block diagram at task (top) level

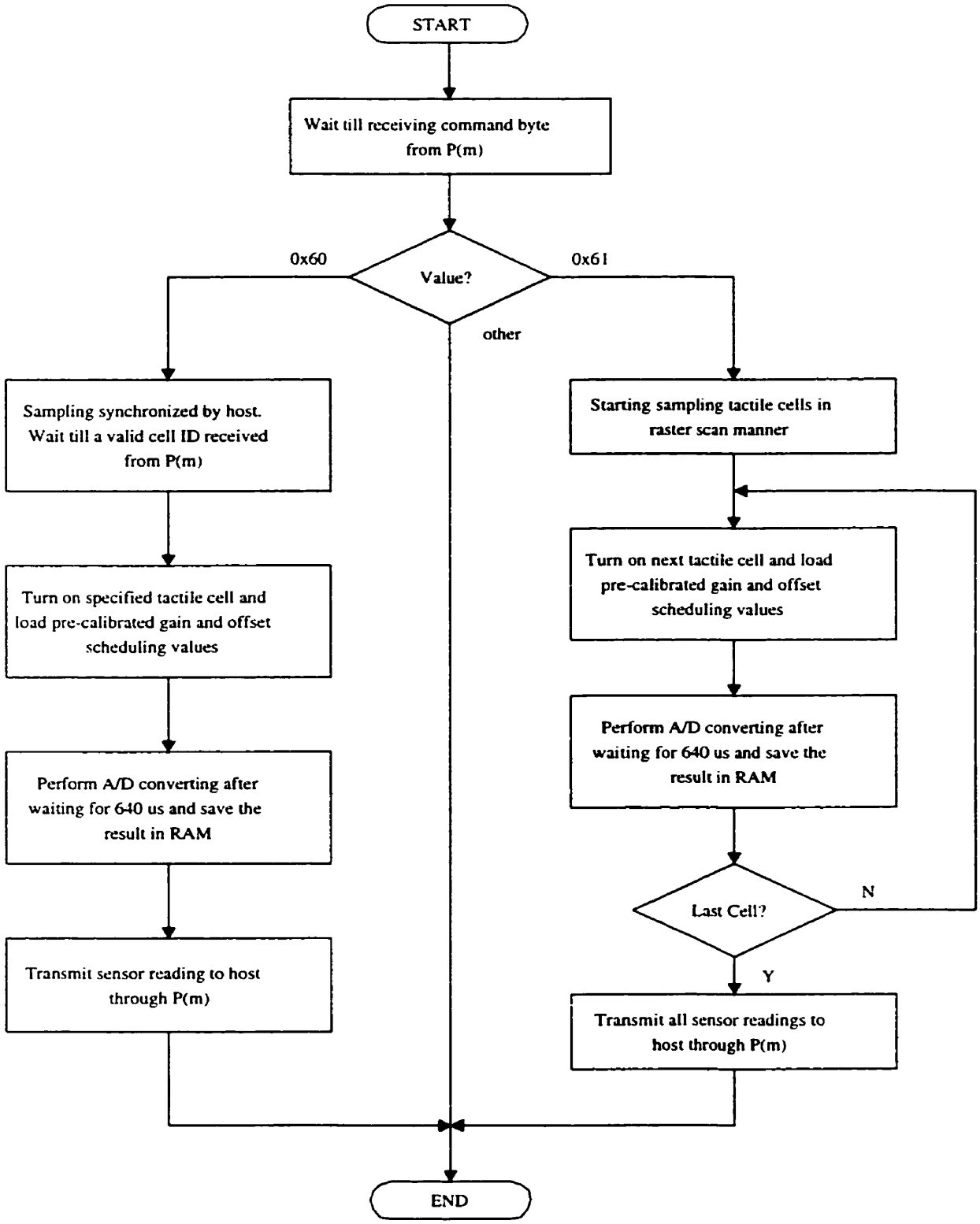

Figure 3.23: Block diagram of application task

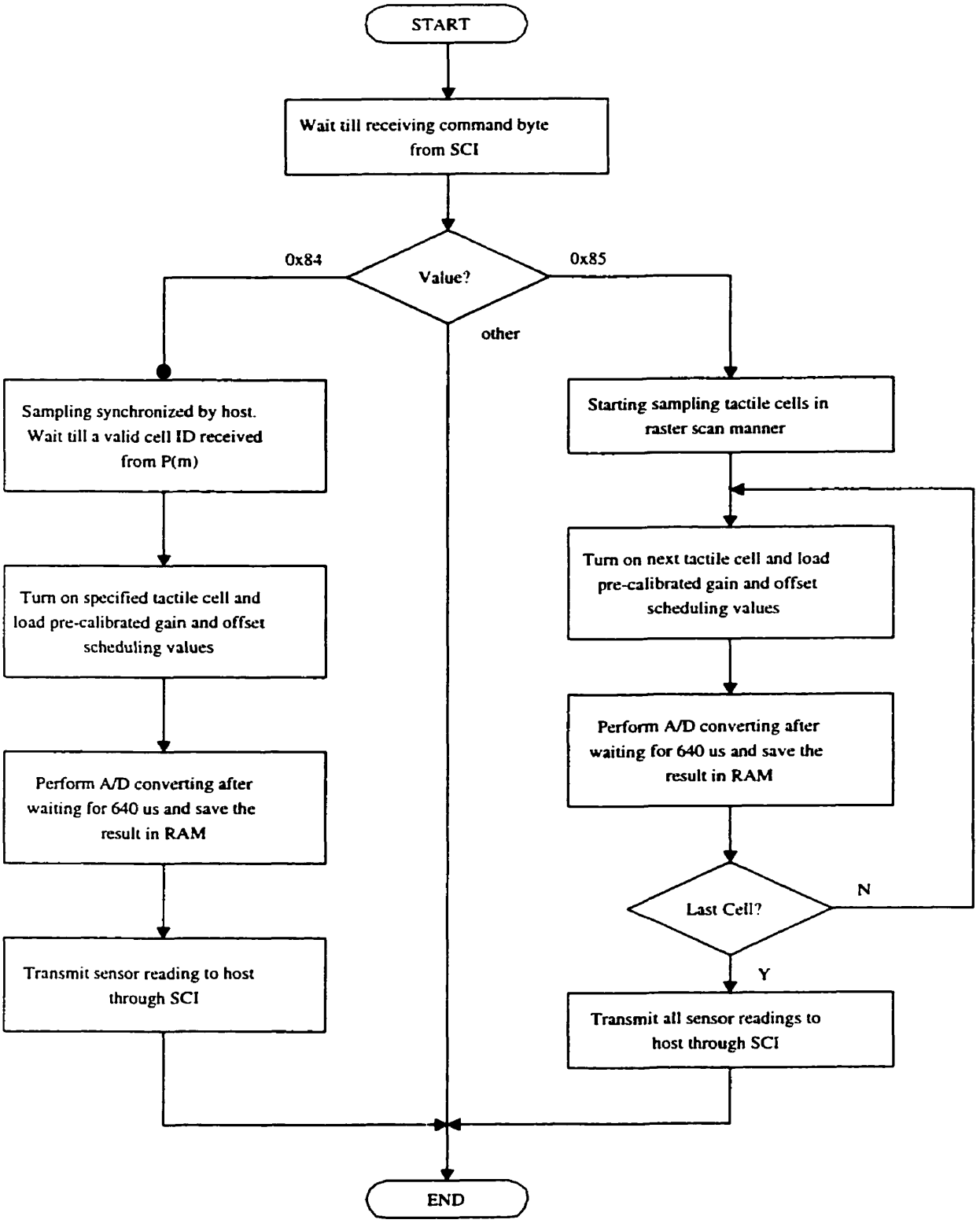

Figure 3.24: Block diagram of demo task

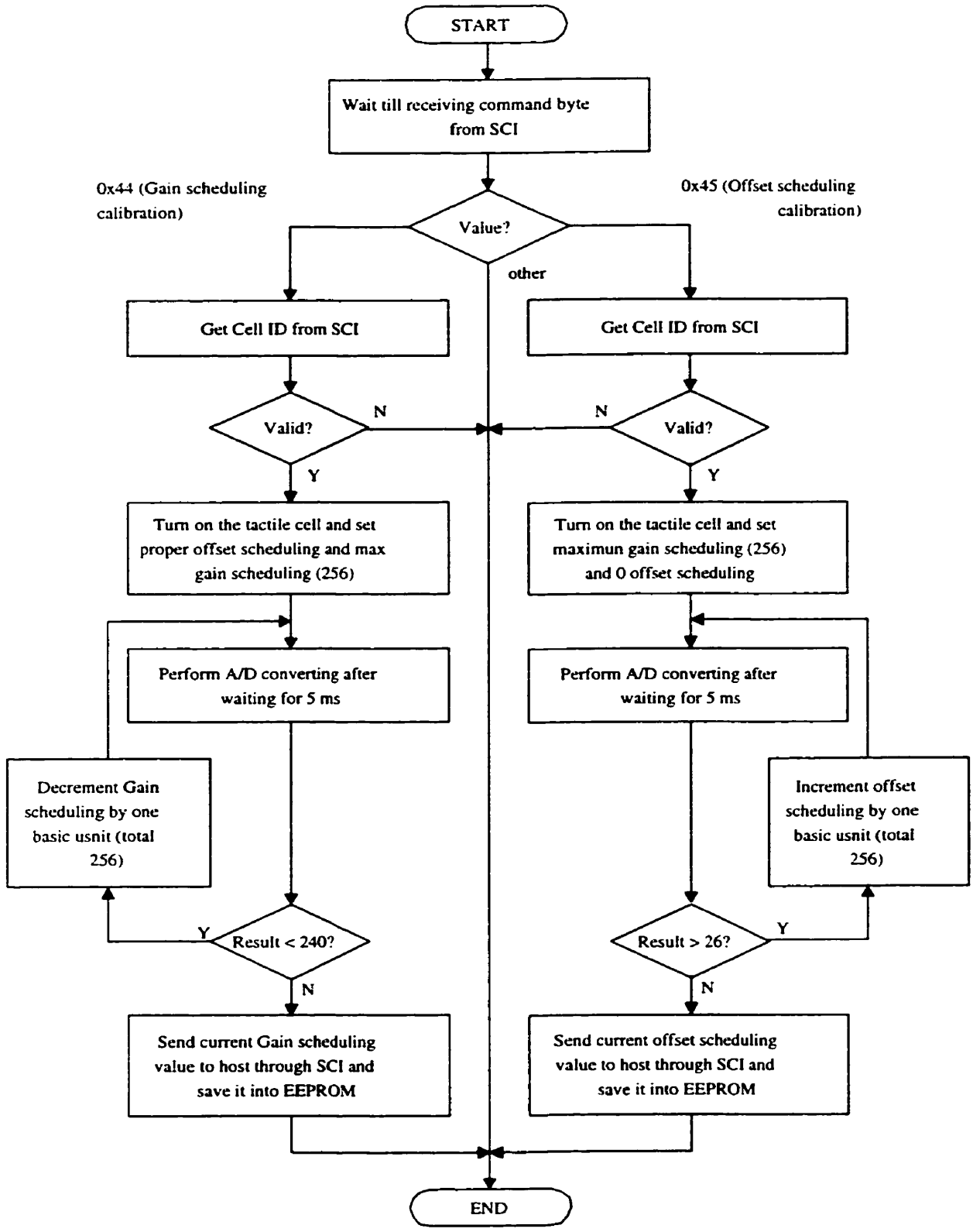

Figure 3.25: Block diagram of testing task

Chapter 4

Experimentation

The experimentation on the Intelligent Gripper System is composed with two aspects. First is the testing and the verification. The major objectives of this part of the experiment are to verify the effectiveness of the various design strategies, and to fully understand the behavior of the system and sensing devices which are difficult to be precisely modeled and predicted. The second aspect is the demonstration of the potential application of the system. Since this thesis is mainly focusing on fundamental issues on the design and the implementation, the demonstration of the application will be relatively preliminary. Besides, the proximity sensor implemented in the current system is modified from the device developed by Petryk and Buehler which has been fully investigated [PB96]. The work described in this chapter is mainly about the tactile sensing subsystem.

4.1 Tactile Sensor Characterization

To understand and model the tactile sensing subsystem, both mechanical and electrical properties have to be identified. The mechanical properties include static, dynamic and spatial properties. The electrical properties include the sensor signal/noise ratio and the sampling rate.

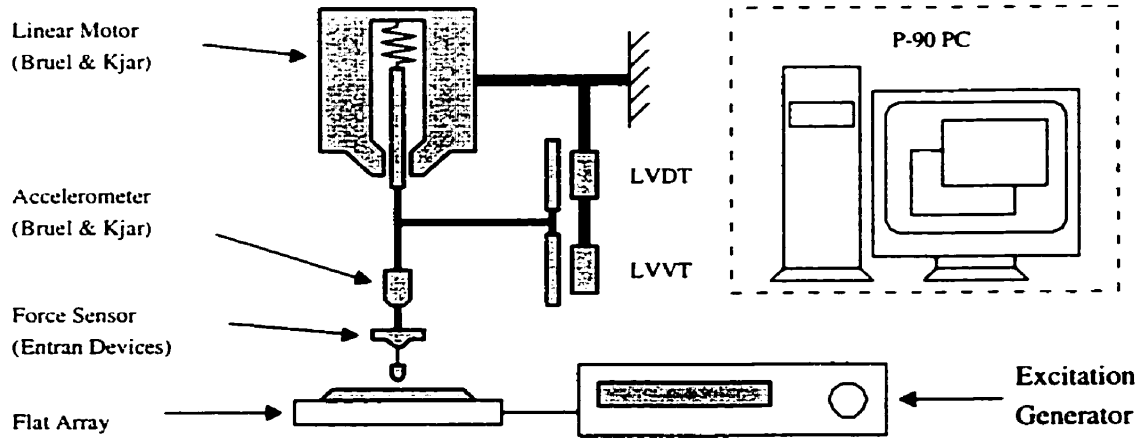

Figure 4.1: Experimental setup

4.1.1 Experiment Setup

The experimental setup is shown in Figure 4.1. A flat palm tactile sensing array identical to which is used in the Intelligent Gripper System is used for testing. A transversed Bruel & Kjaer voice coil linear motor on the top exerts force onto a tactile sensor cell through a $2.5mm$ diameter probe. The tactile array is located under the probe by a three DOF Cartesian stage. A combined LVDT-LVT measures the position and the velocity of the probe. A Bruel & Kjaer force sensor installed between the probe and the motor shaft measures the applied force and a Bruel & Kjaer accelerometer installed right above the force sensor measures the linear acceleration. The vertical position of the probe is controlled by an analog PD controller with an digital input for set point commands.

The mechanical bandwidth of the system is determined by the motor which is around $50Hz$. The sampling and control are provided by a Micron P90 personal computer running Labview software, through a ComputerBoards analog I/O board with 8 channels of 16-bit A/D and 2 channels of 12-bit D/A. The maximum system sampling rate is close to $4.5KHz$.

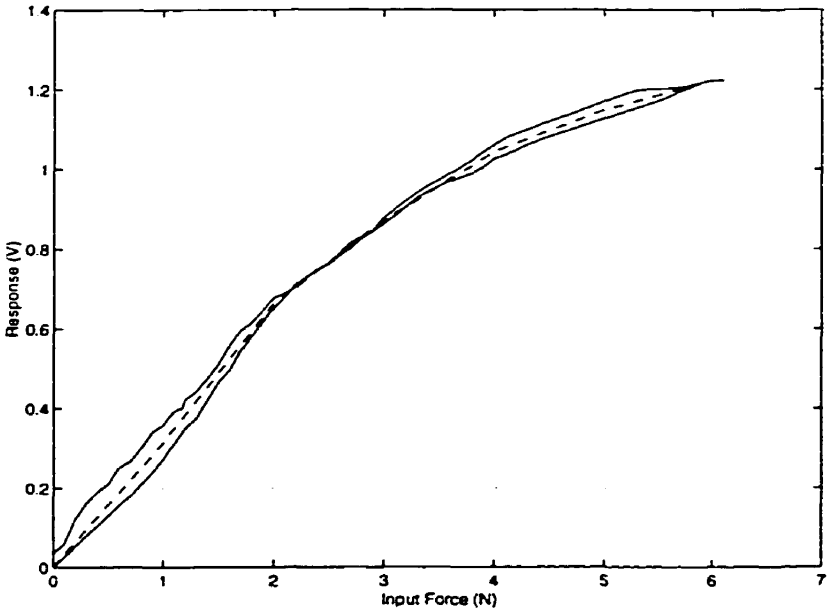

Figure 4.2: Hysteresis loop in the static response of a tactile sensor.

4.1.2 Static Property

One sensor unit in the sensor array (unit 3,3) is experimented with to characterize the static linearity and the stiffness. Figure 4.2 shows the hysteresis loop for moderate forces of up to $6N$, which is roughly the operating range of the sensor. The amount of hysteresis is less than eight percent which is considered small, though the force versus output voltage relation is nonlinear. A segmented straight line fit is employed to model this non-linearity with satisfying results. From the experiment, it is found that the hysteresis curves separate significantly when substantially higher forces are applied. On the other hand, by investigating the relationship between the input force and the compression, it is found that the stiffness of the sensor is around $2.5 \times 10^4 Nm^{-1}$ within its operating range.

4.1.3 Dynamic Property

A single tactile cell can be modeled as a second order mechanical system:

$$y = m\ddot{x} + b\dot{x} + kx \tag{4.1}$$

where x and y are the sensor response and the input force respectively, and stiffness k has already been identified. In the experiment, the probe and the sensor unit have been kept well contacted. The input force measurement is made from the load cell. Therefore the mass m is the total mass of the floating part of the sensor unit and the mass of the probe plus the half of the loadcell which can be precisely measured. The floating part of the sensor includes the floating pad and the top shielding rubber layer. The dielectric rubber layer is very thin and its mass is ignored.

Using the Matlab System Identification Toolbox, it is found the system damping is $1.3 \times 10^2 Nsm^{-1}$ while the sensor mass is no larger than $0.05g$. This is an extremely over damped system and the projected bandwidth is $220Hz$. The swept sine test resulted in a flat response which indicates that the sensor is well beyond the $50Hz$ bandwidth of the actuator.

4.1.4 Spatial Property

The spatial property of the tactile sensor is basically the crossing response over sensor cells in a close neighborhood. To identify this property, the probe is scanned across the surface while the response of a single tactile cell is monitored. Figure 4.3 shows this response in respective to the x-dimension scanning. The contiguous changes of the sensor response with the probe position are due to underlying continuum mechanics of the rubber layers.

One of the most significant applications of tactile sensing is the object localization. To pinpoint more finely the location of the probe, a weighted averaging of responses of neighboring sensor cells scheme is applied:

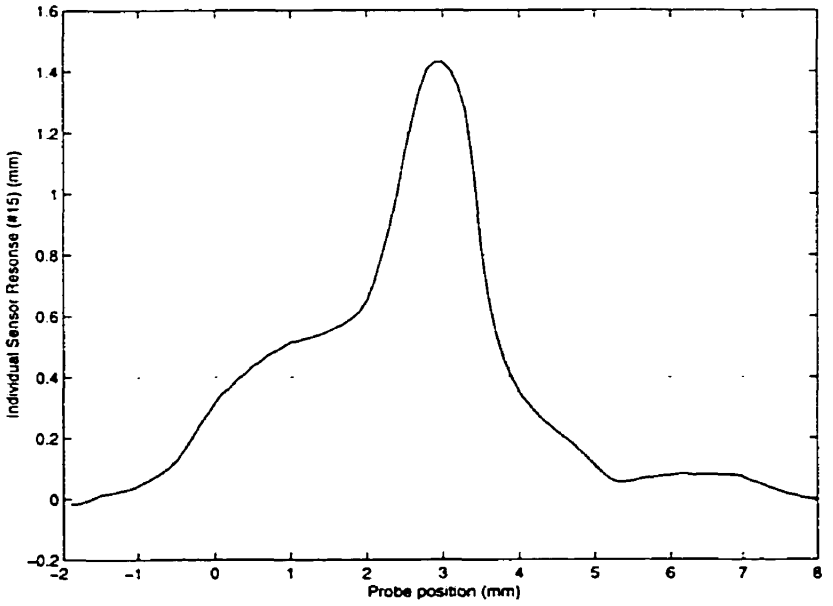

Figure 4.3: Single tactel response to lateral scan

$$y = \frac{\Sigma f_i x_i}{\Sigma f_i} \tag{4.2}$$

where y is the location of the probe while x_i and f_i are the location of the sensor unit i and its output, respectively. In this case, only one dimension is considered but it is sufficient to demonstrate the issue.

The results are also shown in Figure 4.4, which compares the location predicted from Equation (4.2) (dashed line) to the actual position set by the x-y stage (solid line). The localization resolution of the sensor array is about 1.0 mm which is a factor of 2.5 greater than the tactel spacing.

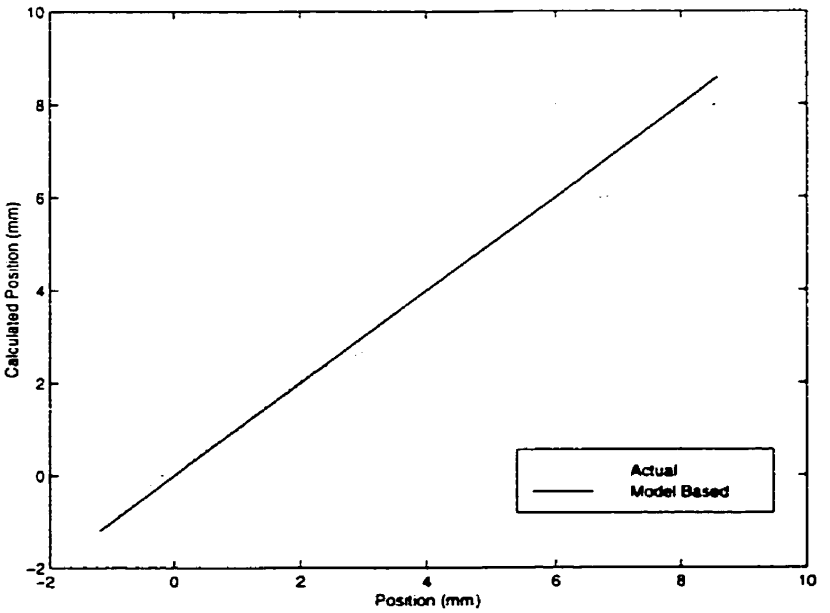

Figure 4.4: Accuracy of point source localization using weighted averages.

4.1.5 Electrical Properties

Noise Level and Sampling Rate

There are two types of electrical noise in the tactile sensor response, the static noise and the dynamic noise. The static noise is contributed by the following sources:

1. The electrical magnetic interference surrounded and coupled by the tactile sensor.
2. The cross interference and coupling from large signal processing circuits to small signal circuits through the power rail and ground.
3. The thermal noise caused by resistors and P-N junctions of the semi-conductor components.

Source 1 and 2 are addressed in chapter3. It is beyond the capability of this thesis to deal with source 3. Besides, the thermal noise level is normally very small and can be ignored.

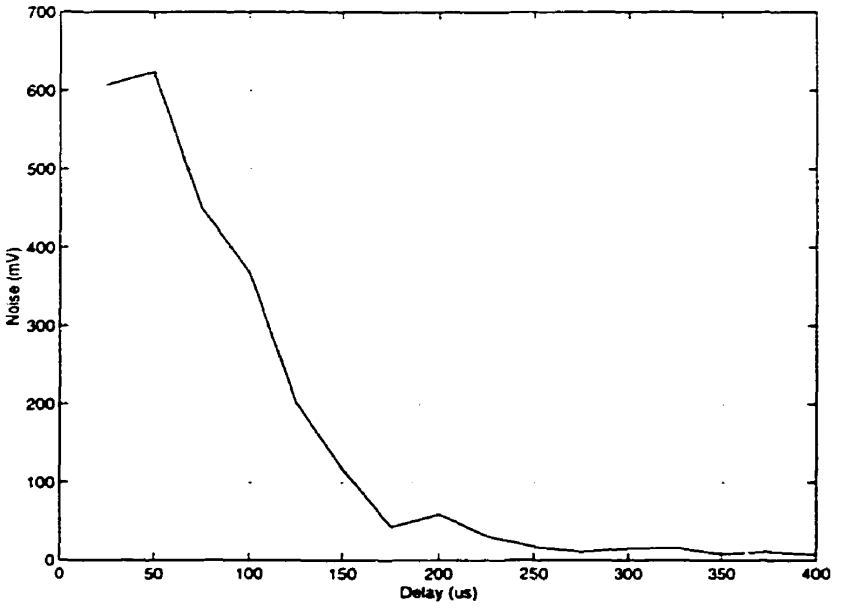

Figure 4.5: Noise level vs. pre-sampling delay for the tactile array

The actual measurement yields a $1mV$ RMS static noise level. For an output range of around $1V$, the dynamic range of the sensor is around 10 bits.

Unlike the static noise whose level is not affected by the sampling scheme, the dynamic noise is contributed by the operation of multiplexor, the electronic switch.

As discussed in Chapter 3.2, the multiplexing circuitry generates strong wide band noise during on and off switch. However, this noise is transient and declines quickly after the switch is stabilized. To obtain reliable sensor readings, the MCU has to wait a period of time after the sensor cell is turned on to proceed the A/D converting. The longer it waits, the better signal quality it will have. This delay actually determines the sampling frequency of the system. Figure 4.5 shows noise level in the A/D readings of cell(3,3) at different sampling intervals. To retain a 7-bit resolution of the sensor response, the maximum sampling rate is $1KHz$ for the individual sensor cell and $15Hz$ for the entire array.

Sensor #1	Normal conductive silicone with silver compound (R-2937).
Sensor #2	Newly formulated conductive silicone with silver-aluminum compound (LSR-9923).
Sensor #3	
Sensor #4	Non-conductive silicone which is identical to that used for the dielectric layer (R-2186).
Sensor #5	

Table 4.1: List of tactile arrays using different shielding materials

In the case where only one sensor cell is being used, the dynamic noise doesn't exist since there is no switching activity.

The Shielding Rubber Layer

The tactile sensors are covered by a conductive silicone layer. The purpose to adopt this layer is based on the assumption that the electrical-magnetic interference caused by metal objects which touch the sensor may introduce a large amount of noise into the sensor readings or even cause the sensor to malfunction.

To investigate how serious this interference could be and what the effectiveness of the shielding layer is, five tactile arrays using three different types of materials for outer-most layer (shielding) have been fabricated and tested (Table 4.1):

The results show sensor #1 has a reasonably good static response on metal objects. However, its performance decays over a short period of time. Four months later, the response on metal objects becomes completely random and the cross talk between individual sensor cells is radical on a global basis (Figure 4.6).

Sensor #2 and #3 essentially behave very much similarly as sensor #1 does. They fail to have any noticeable improvement over sensor #1.

Surprisingly, sensor #4 and #5 have a very good and long-lasting performance (Figure 4.7). First, there has been no noticeable difference observed in noise level when they handle metal objects or non-metal objects (plastic in this case). This provides the evidence that under the current design, the electro-magnetic interference is actually not as bad as originally anticipated. Second, these two sensors are about

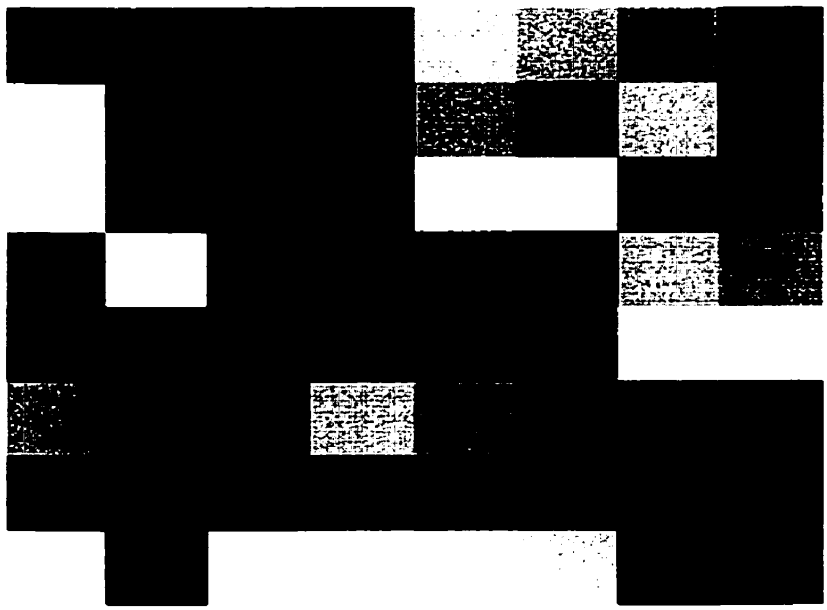

Figure 4.6: Tactile image of a degraded array contacting with an aluminum bar

200 percent more sensitive than sensor #1 to #3. While there will be a discussion in the next chapter trying to analyze and interpret this phenomenon, a comprehensive study is needed for further understanding.

4.2 Using Tactile Sensor in the Contact Force Control

In the robot manipulation, the transient force control has been a challenging issue. Usually the force controller uses the wrist force/torque sensor as a feedback device. Due to the high frequency disturbances caused by the compliance of the sensor and the manipulator itself, the force controller is usually unstable. One of the simplest and the most commonly used methods employs a dominant pole to the system plus low pass filtering to the force feedback signal [XHM95]. The disadvantage of this method is that the bandwidth of the controller is sacrificed.

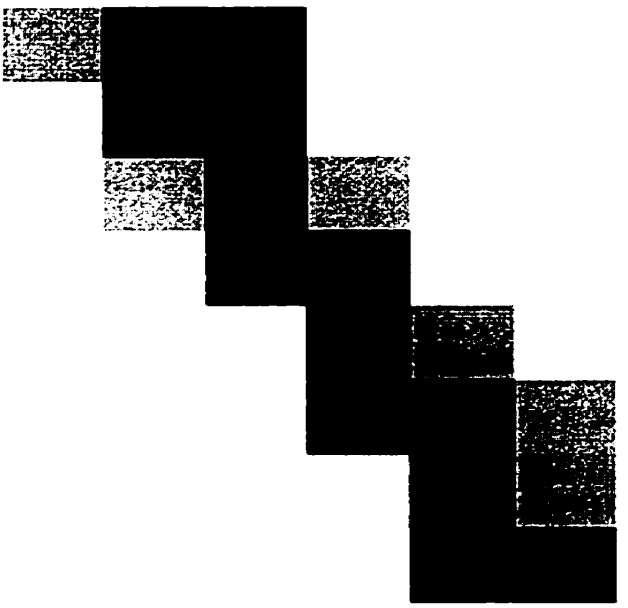

Figure 4.7: Tactile image of a normal array contacting with the same aluminum bar

Because of its dynamic response range for the force sensing, the tactile sensor can be used as the feedback device in the transient force control. In this section, the performance of this control strategy is investigated through experiments.

There are two major advantages to using a tactile sensor as a force feedback device which can result in a much more stable force controller. First, the mass from the sensor to the point of contact is very small and can be neglected. Thus the sensor readings reflect the real contact force instead of the contact force plus the "inertia force" of the manipulator end-effectors in the case of using wrist force/torque sensor feedbacks, which is the major cause to an unstable force controller. Second, the high frequency structure vibration may not be reflected in the tactile sensor readings due to the high damping ratio of the sensor. On the other hand, the non-linearity of the tactile sensor such as the saturation and the hysteresis become significant when large transient forces occur, thereby jeopardizing the performance of the controller and making the system unstable.

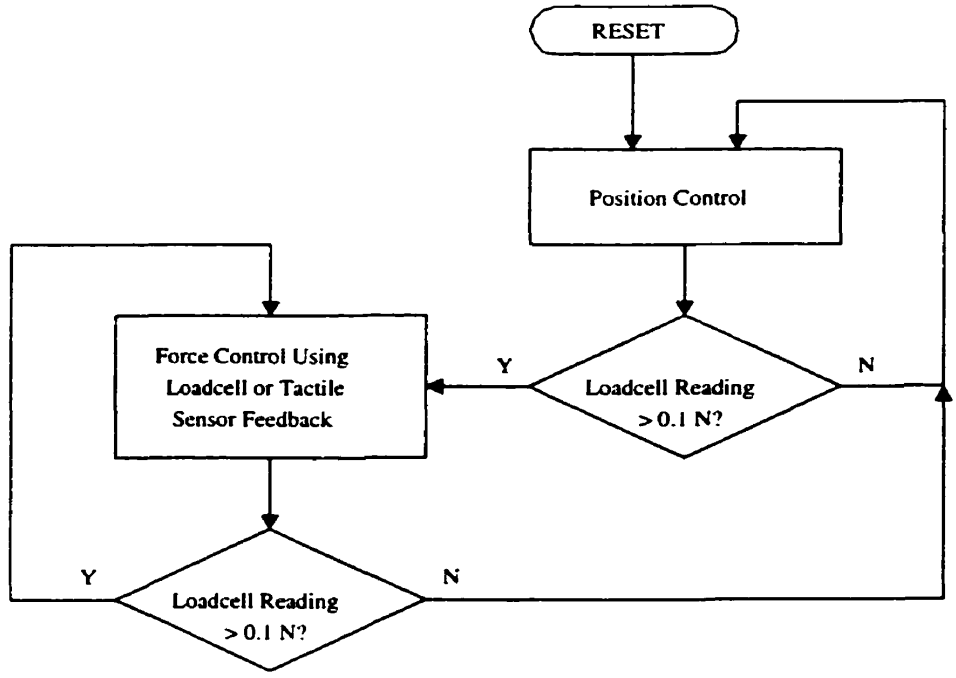

Figure 4.8: Block diagram of a loadcell or tactile sensor based transient force controller

In the experiment, the actuator command is pre-filtered by a first order low-pass digital filter with $100Hz$ cutoff frequency while no low pass filter is applied to either the loadcell or the tactile sensor. The force set point is $3.0N$ and the threshold for position-force switching is $0.1N$. Before the tactile sensor/load cell reading exceeds $0.1N$, the probe keeps moving towards the tactile array through a position PD control using LVDT/LVVT as feed back devices. As soon as the tactile sensor/load cell reading reaches $0.1N$, the control immediately switches to force PD control using either of the tactile sensor or the loadcell as the feedback device. This strategy is depicted in Figure 4.8. Figure 4.9 and Figure 4.10 show the results of the transient force control using loadcell and tactile sensor readings as feedbacks, respectively. The controller using the tactile sensor works well, while the controller using the loadcell is not stable.

A good force controller needs accurate force measurement for feedback. The reason tactile based force control performs better is simply because the tactile sensor generally

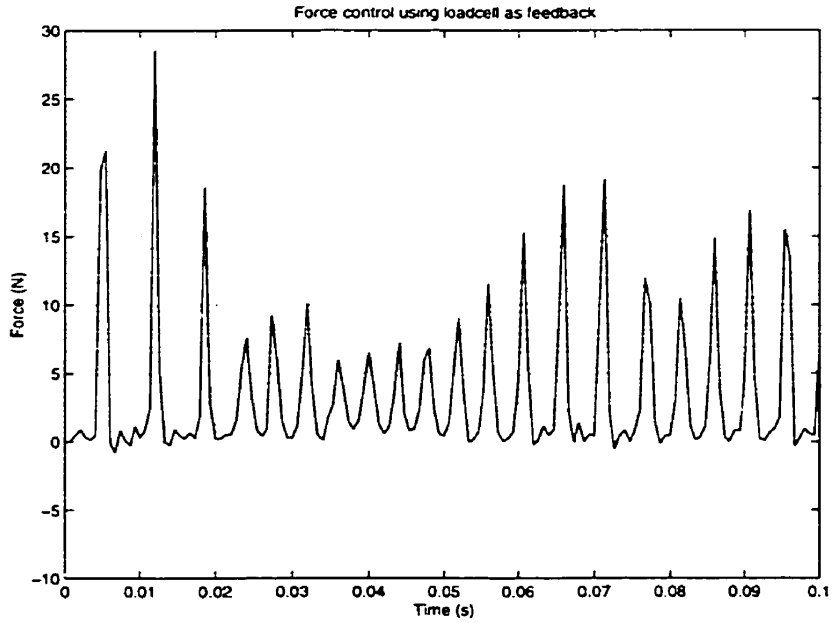

Figure 4.9: Transient force control with loadcell feedback

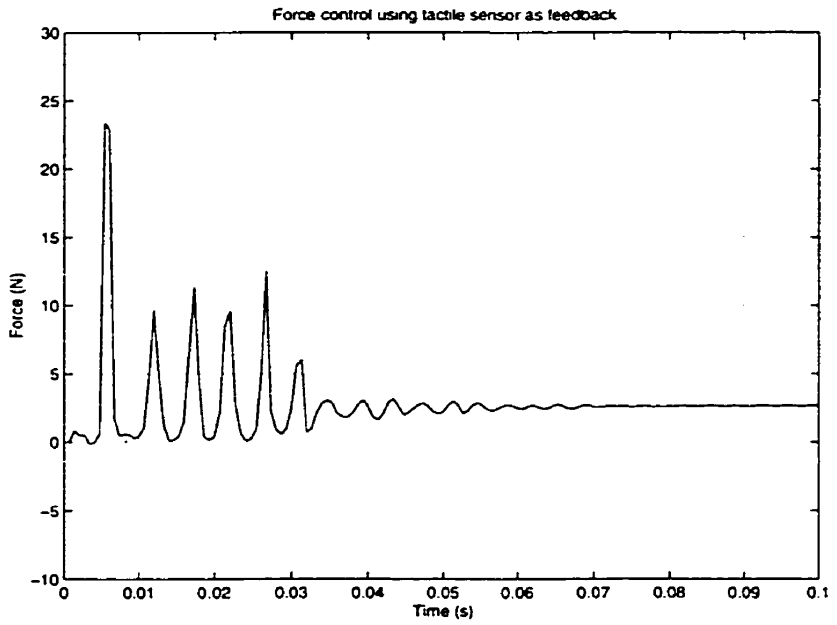

Figure 4.10: Transient force control with tactile sensor feedback

records actual contact force more precisely. However, this may not be always true. Based on the fact that the tactile sensor gets saturated and larger hysteresis appears in the response when large transient force occurs, the tactile sensor could be doing a worse job. So why not switch back to the loadcell under such situation? Based on this argument, a modified PD controller employing both the loadcell and the tactile sensor is tested. The controller simply switches to the loadcell from the tactile sensor when the reading from the tactile sensor is beyond a threshold and switches back as soon as the reading was below it. In this case, the threshold is $5.0N$, a turning point beyond which the tactile sensor starts to be saturated. Figure 4.11 demonstrates the control law graphically and Figure 4.12 shows the results. It is obvious that this strategy results in a better controller compared to Figure 4.9 and Figure 4.10.

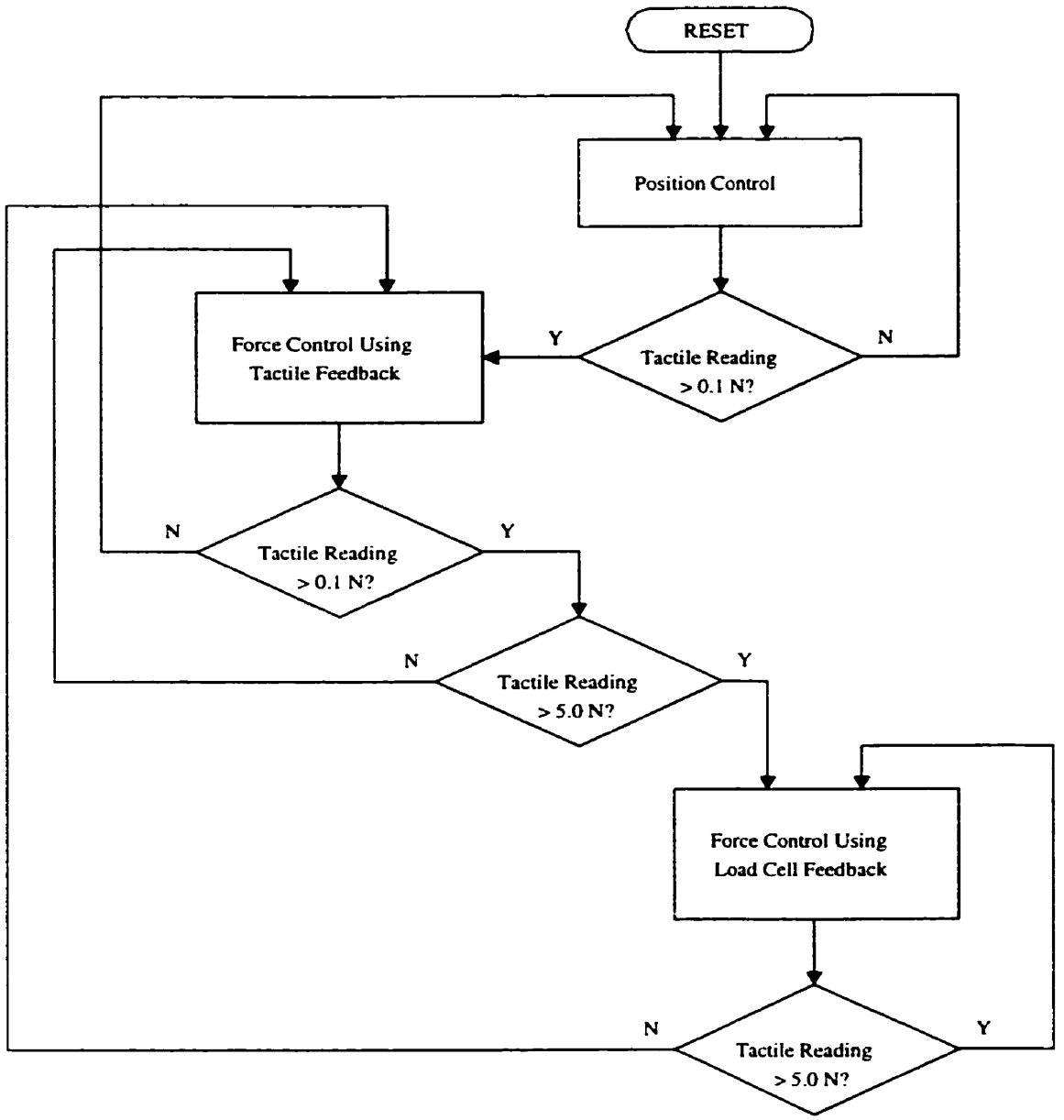

Figure 4.11: Block diagram of a transient force controller with composite tactile sensor/loadcell feedback

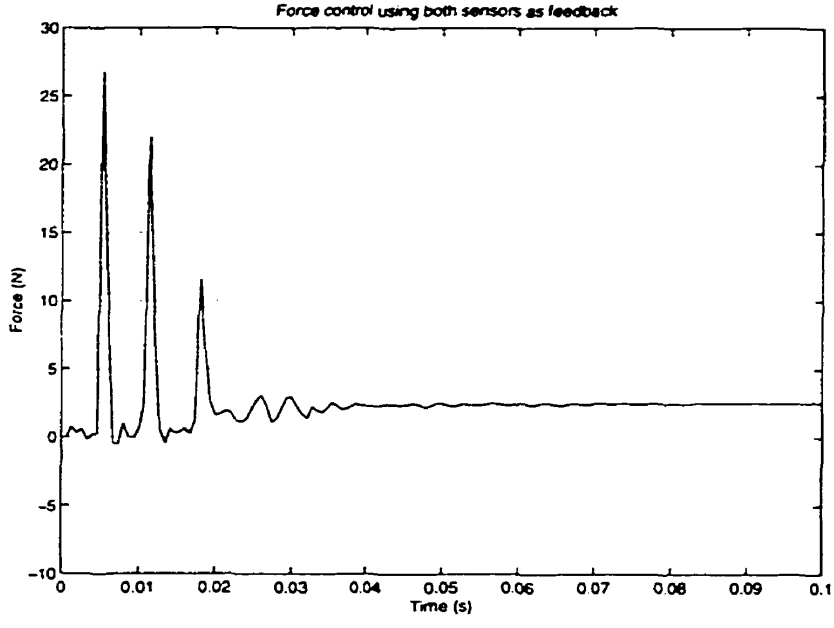

Figure 4.12: Transient force control with composite sensor feedback

Chapter 5

Discussion and Conclusion

5.1 The Conductive Silicone Shielding

The idea of using conductive silicone in the top layer of a tactile array is to form a shielding which reduces the electrical-magnetic interference. Because of the limited tools and highly complicated nature of the materials being used, an ideal shielding layer is never guaranteed. It is interesting to observe that the use of this material does not always have the positive impact on the sensor performance. In our case, experimental results also show the EM interference does not cause noticeable damage to the sensor reading. This is possibly due to the relatively large size of individual tactile cell.

The "conductive silicone" is actually the pure silicone which is a non-conductive compound mixed with tiny silver (R-2937) or silver-aluminum alloy balls (LSR-9923) whose maximum diameter is around $50\mu m$. The density of these metal balls is high enough to let them have constant contact to each other. The material therefore has a very good conductivity but obviously it is not homogeneous compared to metal.

Figure 2.1 illustrates the basic electrical model of a tactile sensor. Things get a little more complicated when the sensor is covered by a conductive silicone layer. There are two additional parasitic capacitors introduced in this case and they will possibly

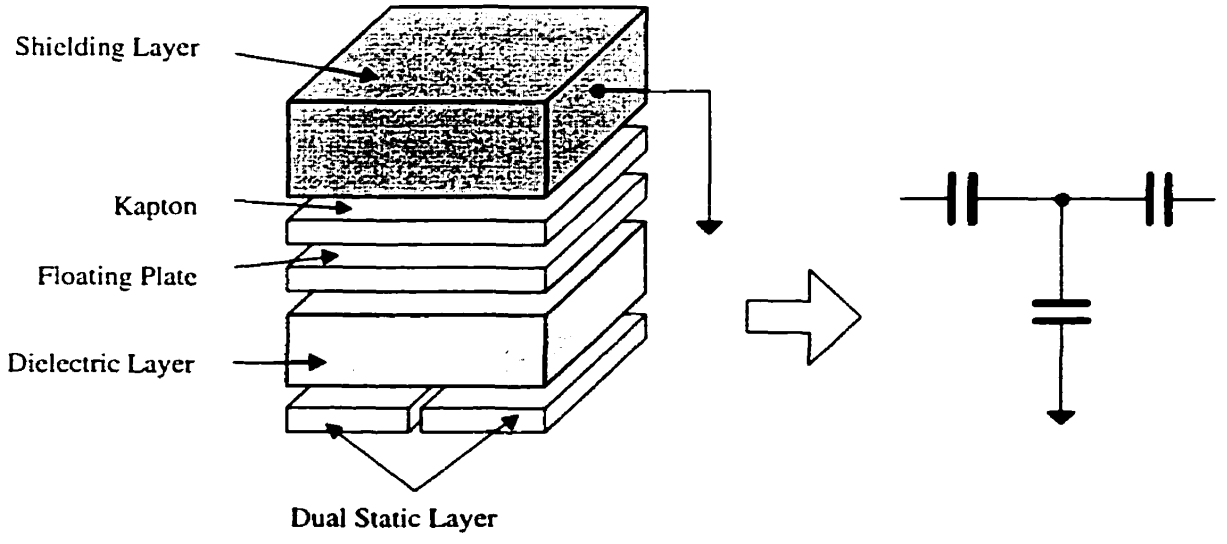

Figure 5.1: Tactile sensor with conductive shielding and its electrical model

cause a deterioration to the sensor performance.

Figure 5.1 is the cross view of the new configuration and its effective electrical symbolic representation. The basic capacitor measurement unit is evolved into Figure 5.2.

C_1 and C_2 are tactile sensing capacitors whose values are $0.5pf$ according to Equation (2.1) . Due to the presence of the conductive layer, an additional capacitor C_g is generated between the floating plate and the ground. The idle state sensor response is:

$$V_{out} = 2\pi f V_e R \frac{C_1 C_2}{C_1 + C_2 + C_g} \tag{5.1}$$

Because the dielectric media of C_g is the 2-mil thick kapton whose dielectric constant is relatively large (5.0), its capacitance could be much larger than the C_1 and C_2, though its actual value depends on the micro-structure of the conductive layer which is unclear and difficult to model. C_g causes a short to the signal and contributes nothing to tactile sensing since it doesn't change when the sensor is loaded. In the

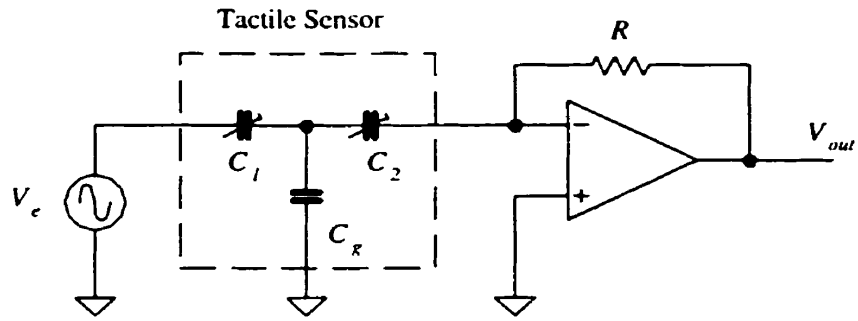

Figure 5.2: Modified tactile sensing unit

worst case, C_g can be as larger as:

$$C_g = \epsilon_0 \epsilon_r \frac{A}{d} = 8.85 \times 10^{-12} \times 5.0 \times \frac{(2.54 \times 10^{-3})^2}{0.002 \times 25.4 \times 10^{-3}} = 5.7(pf) \tag{5.2}$$

which results in an attenuated sensor response of:

$$V_{out} = 2\pi f V_e R \frac{0.5 \times 0.5}{0.5 + 0.5 + 5.7} = 0.075\pi f V_e R \tag{5.3}$$

While in the the best case where C_g does not exist, the sensor response is:

$$V_{out} = 2\pi f V_e R \frac{0.5 \times 0.5}{0.5 + 0.5} = 0.5\pi f V_e R \tag{5.4}$$

Comparing (5.4) with (5.3), the sensor could be 5.7 times more sensitive using non-conductive silicone. This may explain the result from the experiment. On the other hand, from the fact that a sensor with a non-conductive top layer is two hundred percent more sensitive, C_g can be calculated:

$$\frac{C_1 + C_2 + C_g}{C_1 + C_2} = 3.0 \;\Rightarrow\; C_g = 2(pf) \tag{5.5}$$

More serious problems occur when the conductivity of this shielding is degraded which is observed over a period of time after the rubber has cued. Under such a situation the grounding of this shielding layer could become very poor and even broken

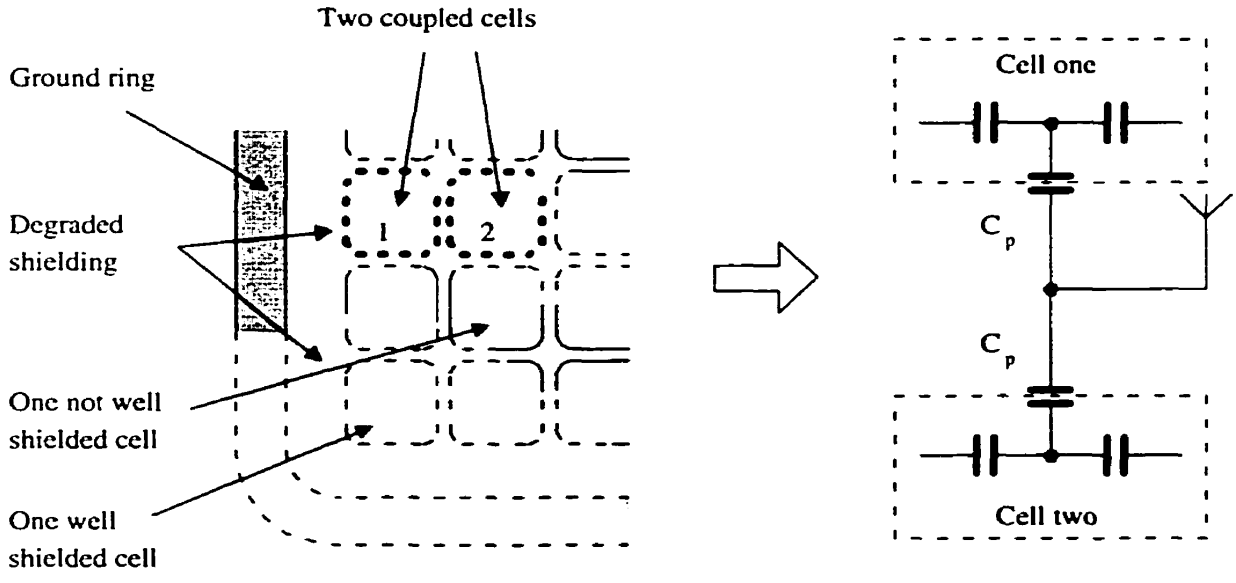

Figure 5.3: Illustration of a tactile array with degraded shielding and its electrical model

(this could happen due to the limited contact between shielding layer and the PCB ground ring). In this case, the shielding layer becomes a large floating conductive layer or a set of isolated conductive islands floating on the top of kapton as shown in Figure 5.3.

The shielding becomes an "antenna" and is closely coupled with the floating plates through C_p, the second parasitic capacitor. The "antenna" introduces huge noise and dramatically changes the entire electrical characteristic of the sensor when the sensor makes a contact with a metal object, which is often remotely grounded through a very large loop. Notice that C_p is distributed all over the sensor array, the noise introduced from one contact location may cause a false sensor response at a distant location. Viewing from the output of the entire array, this appears as a radical cross talk as observed from the experiment (Figure 4.6).

In the case of non-conductive silicone top layer, this "antenna effect" is highly reduced because this out-most layer is 20 times thicker ($40mils$ vs. $2mils$) therefore

the coupling between the floating plate and the metal object can be reduced. This may explain why the performance of the sensor with the conductive silicone shielding gets worse after being used for a certain period of time. It is unclear how the silicone loses its conductivity. It could be caused by the changes of chemical characteristics of the material or caused by fatigue of the rubber.

Based on above arguments and experimental results, it is clear that a poor shielding is worse than no shielding at all. Since the conductive silicone is not a homogeneous conductive material, it is not guaranteed that the entire piece is always well grounded. The "antenna effect" exists more or less depending on its condition. The internal micro structure of this material is unclear and complicated therefore is very difficult to model. While the fully understanding of this phenomena is a further research topic, the sensor with normal non-conductive silicone top layer works extremely well and is adopted in the current design.

5.2 Future Work

The work covered in this thesis is the research and development of a rubber based tactile sensing array and all the essential supporting hardware and software. Combining an infrared proximity sensing array, the Intelligent Gripper System is composed. A tactile sensor based force control scheme is also investigated. Based on these achievements, more research is able to be conducted.

5.2.1 Application of the Intelligent Gripper System

The robot manipulation based on both tactile sensors and proximity sensors remains an very interesting topic in the future. A typical experiment could have a robot, for example, a Sarcos Dextrous Slave Arm equipped with the Intelligent Gripper to track, grasp and manipulate an object in a planned manner. The moving object is plastic or fragile which only sustains small forces.

The experiment has three phases. Each of them should be studied separately.

During the tracking phase, the gripper position/velocity controller uses infrared proximity sensors to retain the location and orientation of the object, though this information is normally not very accurate due to the nature of the proximity sensor. At the end of the tracking phase, the gripper is ready to perform grasping at a planned location and orientation.

During the grasping phase, both sensors are used. The controller uses the proximity sensor as the feedback before the contact occurs and the gripper is under the position control. Meanwhile, the controller monitors the tactile sensor response to detect the occurrence of the contact. As soon as the contact occurs, the control switches into the transient force control immediately using feedbacks from the tactile or tactile/loadcell pair. The controller will normally switch between the position control and the force control a few times until the grasping is stabilized.

The third phase is the manipulation which actually involves activities described in the tracking and grasping phases. The gripper may release and re-grasp the object on a constant basis. The management and utilization of tactile and proximity information is critical. Further study may be focused on optimized grasping in which case, the object surface information observed by tactile sensors is used to develop an optimized surface to surface grasping.

5.2.2 Sensor Improvements

While the current tactile sensor meets the specifications and fulfills the requirement during normal operations, there are a number of issues to be addressed which may further improve the performance.

First is the spatial resolution. The spacing of the current design is $2.54mm$. Though a $1mm$ spatial resolution is achieved by analyzing the sensor response from the neighborhood cells 4.2, this scheme is only valid for large object localization. The sensor array is not able to identify or to locate objects smaller than 2.54 mm in an accurate

manner. The tactile resolution of the human finger is about 1 mm [PJ81]. In order to achieve this performance, the density of the tactile sensor matrix over the array has to be increased considerately.

However, this approach reduces the physical dimension of an individual sensor cell by the order of two and results in a proportionally smaller sensing capacitance. Not only is it more difficult to measure a smaller tactile capacitor but also, in this case, the noise introduced by environment interference will be more visible. One approach is to find new material with larger dielectric constant for dielectric layer to compensate the loss of sensing capacitance. Nevertheless, to improve the resolution of a tactile sensor in this category is a big challenge to researchers.

The second issue is the non-linearity in the sensor response, the hysteresis in particular. It is suspected that the kapton is the major cause of this problem. While the silicon used in the dielectric layer has an excellent elasticity, the kapton which hosts the floating plate recovers from deformation very slowly. A large contact force may even bend it permanently. The use of thinner and more compliant kapton will be a good solution though the kapton thinner than 2 *mil* (which is used in the current design) has not been seen in the market. The best solution is to get rid of this kapton completely. But this approach raises the question of how to implant the floating plates.

The third issue is about the conductive silicone shielding layer. A bad conductive top layer will jeopardize the sensor performance dramatically. Though in the current design, a shielding layer is not a necessity, it may be mandatory if the size of an individual tactile cell is reduced since the signal/noise ratio will be worse. To find an excellent compound of conductive silicon is a challenging job but will definitely contribute a great deal to the tactile sensing research.

5.3 Conclusion

In this thesis, the Intelligent Gripper System as a product prototype is presented. The system integrates a rubber based tactile sensing array and an infrared proximity sensing system with the complete supporting and interfacing electronics into one standalone and portable package. Though the system is specifically designed for the Sarcos Dextrous Arm, it is ready to be adapted or recast to other robot end effectors due to its modular and portable approach.

The Intelligent Gripper System is composed with three functional modules. The tactile sensing subsystem module integrates a tactile array and its supporting electronics. The 8×8 tactile sensor array is based on the capacitance measurement and constructed with multiple rubber layers. To achieve goals of robustness, manufacturability and low cost, the tactel spacing is designed as $2.54mm$. As a result, at least two tactile sensor arrays with very good working order have been built. In order to reduce the nonlinearity in the sensor response and extend the life of sensors, a floating conductive layer configuration instead of conventional strips has been successfully adopted. To reduce the noise in sensor response, the supporting electronics including pre-amplification and multiplexing is completely localized in the form of a solid-state part.

The infrared proximity subsystem is based on the LED/photo-transistor pair, the device developed by Petryk and Buehler [PB96] though the associated electronics is specially designed to support four sensing channels. The sensor head including the LEDs and photo-transistors are integrated into the gripper finger along with the tactile sensing subsystem. To simplify the design one LED excitation is shared by two sensing channels. All the associated electronics is packed into one small printed circuit board which can be easily installed anywhere close to the finger tip.

The interface module performs a role as an electronic and data hub for two sensor subsystems and the master controller. The module is based on an MC68HC11 microprocessor (MCU) which makes the whole system "intelligent". The analog signal from

both sensors is converted to digital signal by an 8-bit on-chip A/D converter before being further directed to the master controller through a universal bi-directional parallel port. An external on-board analog to digital converter offering 14-bit resolution is also available and can be used for analysis. There are two additional digital to analog converters which serve as gain and offset schedulers to eliminate the static offset in the sensor response and to normalize the signals before converting them into digital signals. The interface module also accepts commands from the master controller through the parallel port to configure and to trigger the sensing operation. The MCU also allocates the necessary hardware resources to perform a possible low level digital data processing in the future applications. Since all small signal processing circuits are strictly localized or constrained into the two subsystems, there are only digital signals and large analog signals exchanged among three modules, the system has an optimized Electrical-Magnetic Compatibility (EMC).

As a by-product, a Windows based development and evaluation system for the MC68HC11 based embedded system is developed. It is a powerful tool for similar system research and development and has potential commercial value.

There are three parts of experiments conducted in the thesis. First is the evaluation and the verification of all the electronics and programs running in the MCU. It insures that all the issues raised in the design stage are addressed. The overall electronic design is proved successful.

The second part of the experiment is to evaluate and characterize the tactile sensor in terms of electrical properties such as noise level and maximum sampling rate, and mechanical properties including static, dynamic and spatial performances. Under current design, the tactile sensor cell can be sampled as fast as $1KHz$ ($13Hz$ for the entire array) with $1mV$ noise in $1V$ range. The sensor has a small 7 percent non-linearity with a composite $1mm$ spatial resolution, although the tactel spacing is $2.54mm$. The sensor can be modeled as a second order system with $220Hz$ bandwidth.

The third part of the experiment is a preliminary investigation on the use of the

tactile sensor in the transient force control. It has been shown that the contact force is better controlled through less-local joint force/torque sensors. Furthermore, a composite tactile-joint force/torque sensor based force control strategy has been proposed. It yields the best performance, as the dynamic range could be divided between them. These results further support the argument of the utility of tactile sensors.

Finally, the effectiveness of the conductive shielding layer on the top of the tactile array and how it affects the sensor performance have been addressed. Though it is more on the theoretical basis, this will certainly help to further improve the sensor performance in the future.

Appendix A

Materials used for Tactile Array

1. R-2186. Non-conductive silicone used for dielectric layer and top layer. Nusil Silicone Technology Inc. (1050 Cindy Lane, Carpinteria, CA93013).

2. R-2937. Silver based conductive silicone used for shielding layer. Nusil Silicone Technology Inc. (1050 Cindy Lane, Carpinteria, CA93013).

3. LSR-9923: Silver-aluminum based conductive silicone used for shielding layer. Nusil Silicone Technology Inc. (1050 Cindy Lane, Carpinteria, CA93013).

4. Tactile base PCB. 65 mil - 85 mil, available from local PCB manufacturer.

5. Kapton layer. 2 mil, available in local PCB Manufacturer.

Appendix B

Schematics

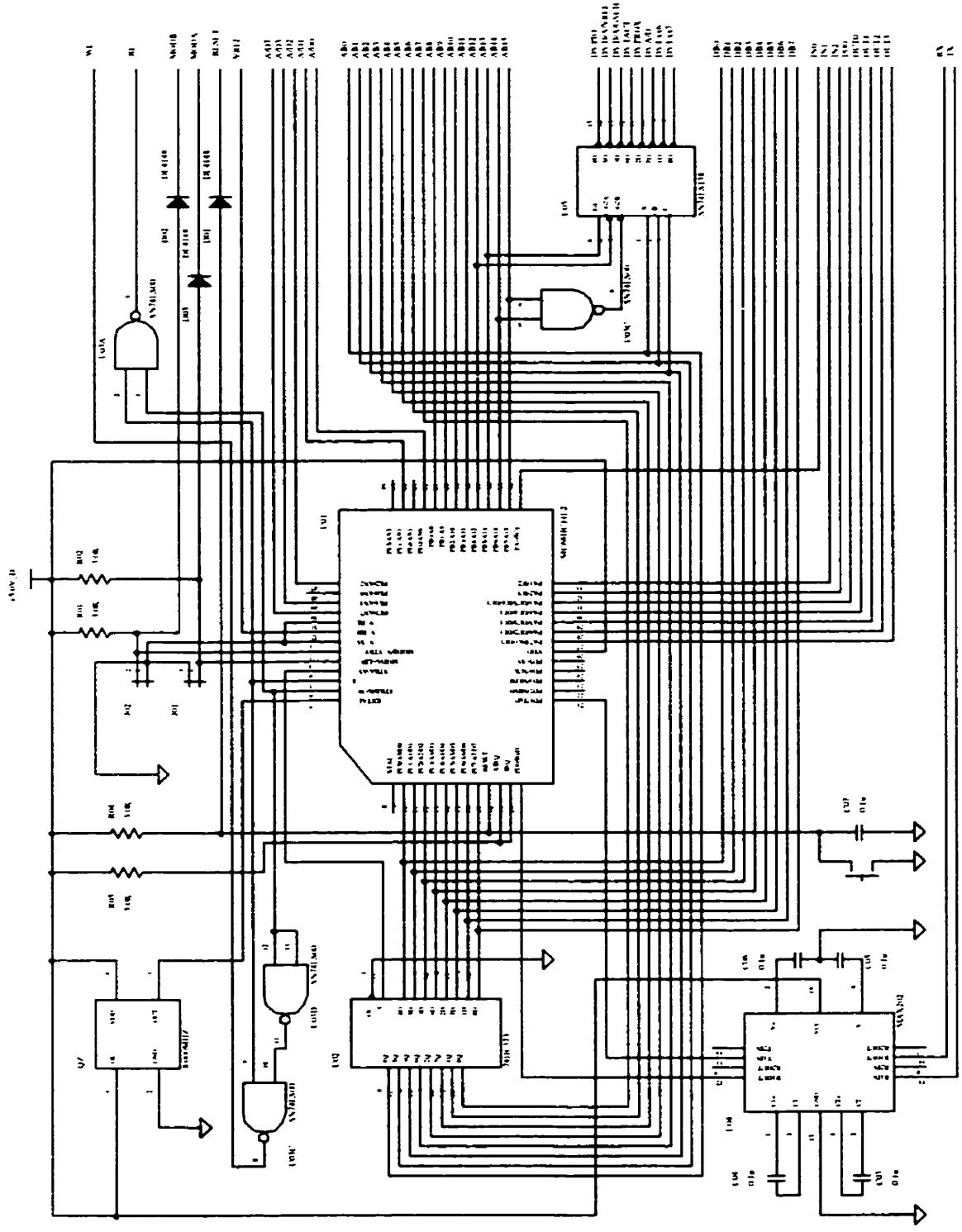

Figure B.1: Interface module: MCU, address decoding and SCI

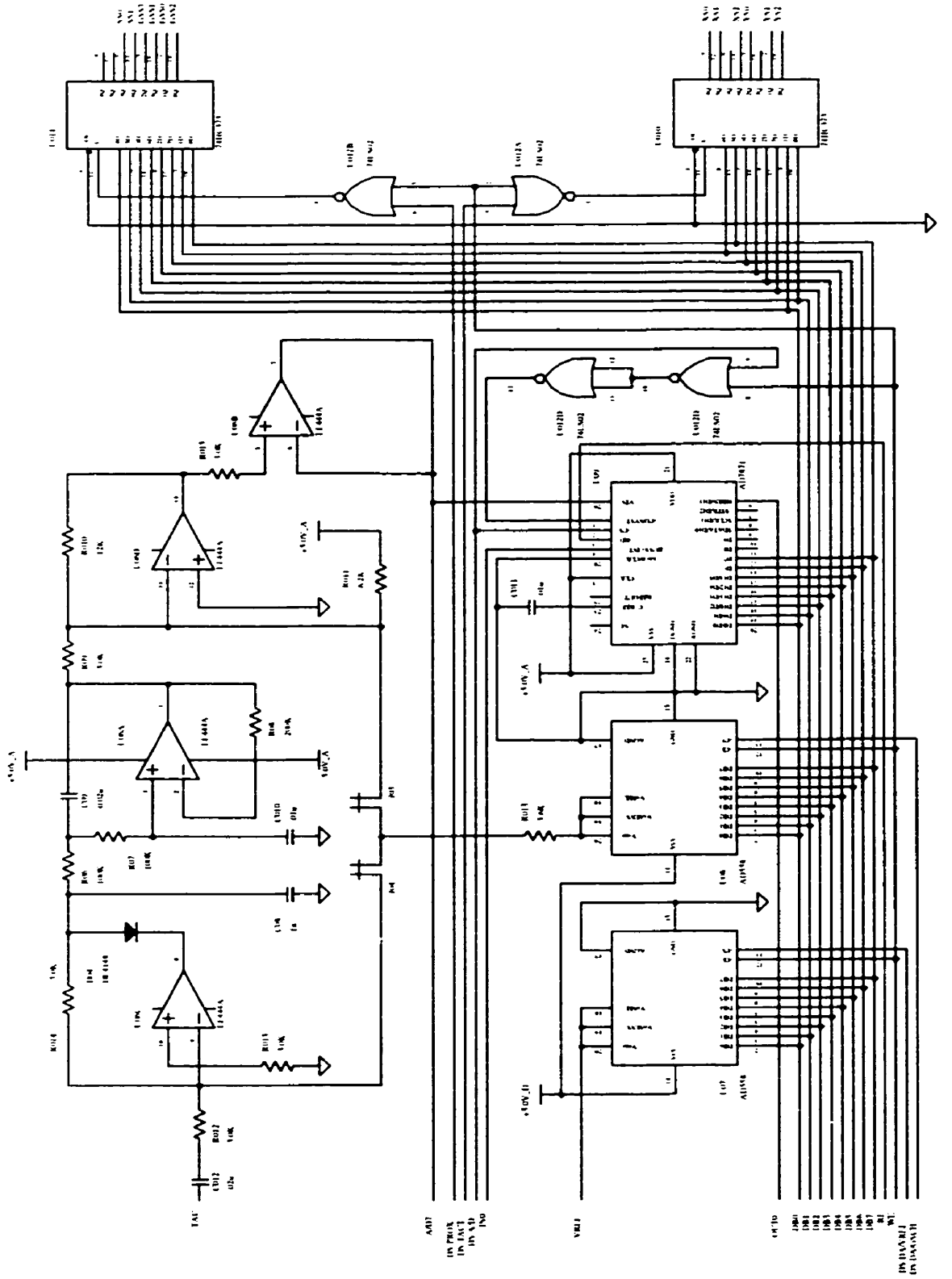

Figure B.2: Interface module: P_t, P_p and tactile signal processing

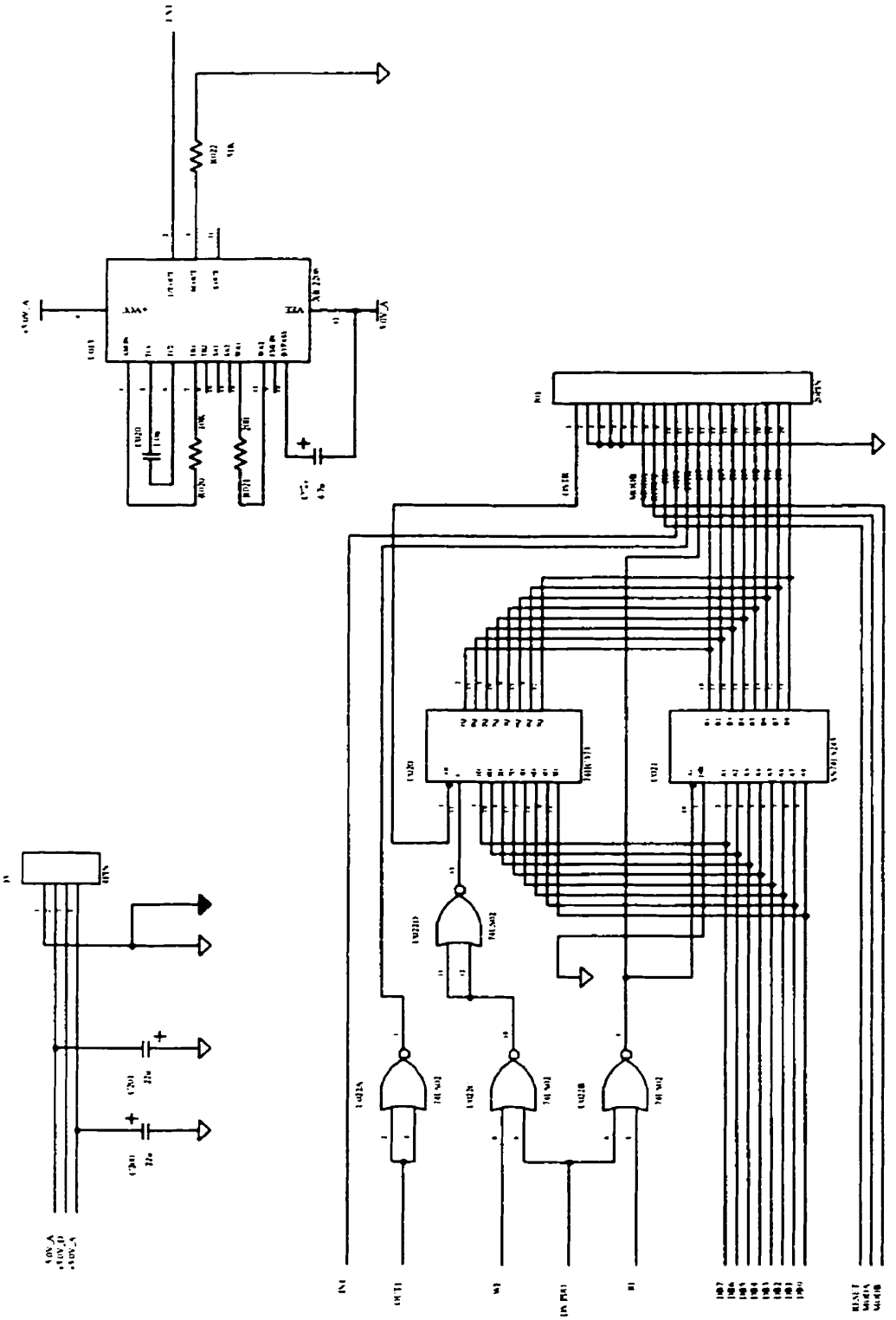

Figure B.3: Interface module: Excitation generation and P_m

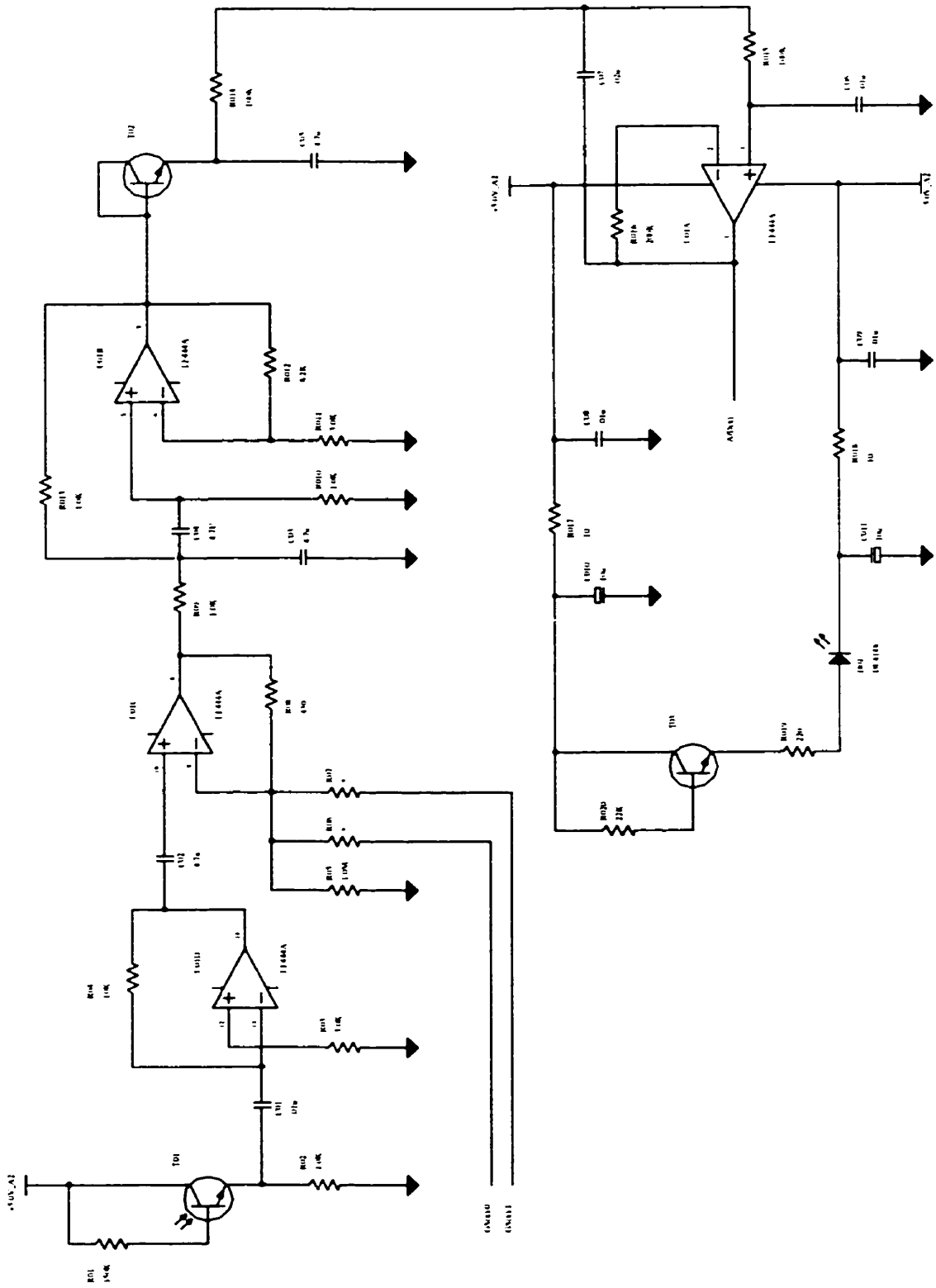

Figure B.4: Proximity subsystem: All analog processing and excitation driving. (One channel is shown. The rest three are identical)

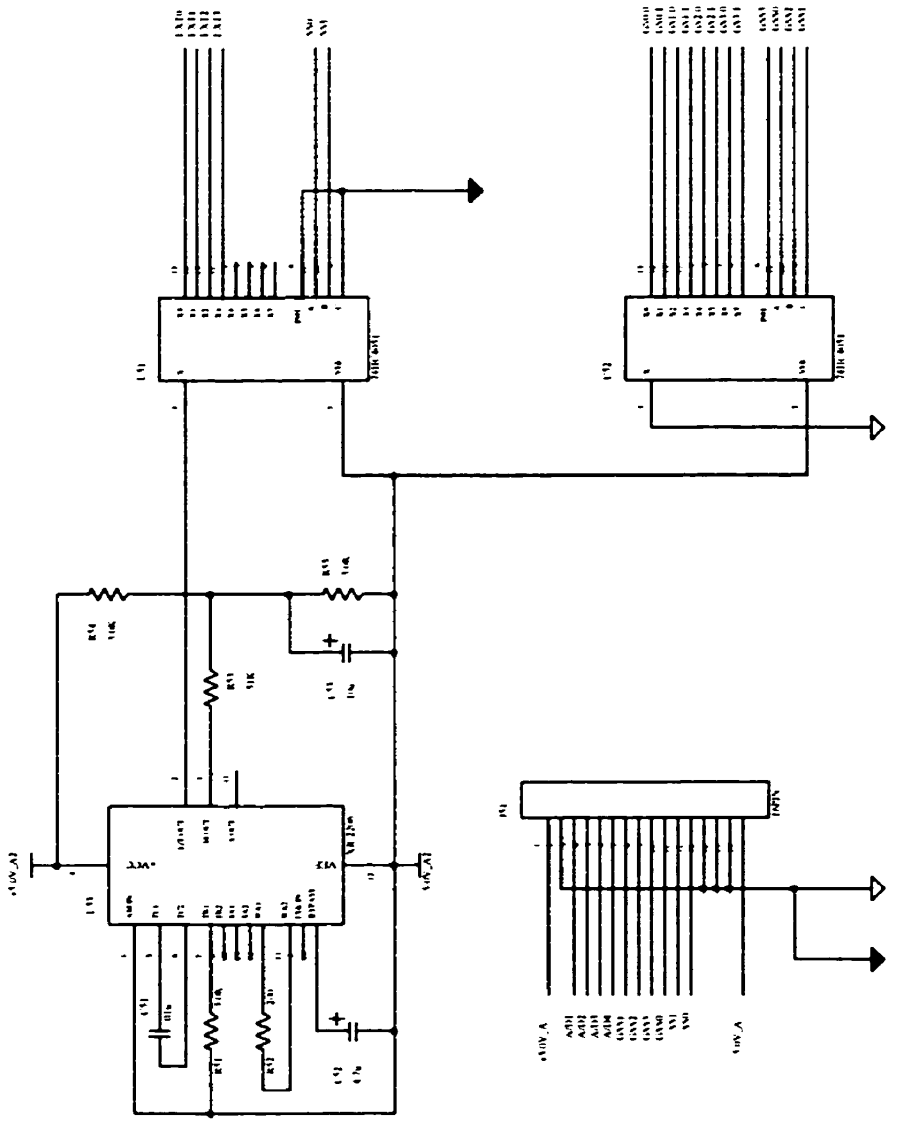

Figure B.5: Proximity subsystem: Excitation generation and multiplexing, gain scheduling control

Appendix C

Lists of the MC68HC11 Program

Due to the limit of the space, lists of the MC68HC11 Program are available upon request.

Bibliography

[Asa86] Kazuo Asakawa. Robot assembly of precision parts using tactile sensors. *Advanced Robotics*, v. 1 n. 1:59–69, 1986.

[BK91] Alan D. Berger and Pradeep K. Khosla. Using tactile data for real-time feedback. *International Journal of Robotics Research*, v. 10, n. 2:88–102, 4 1991.

[Boi84] R. A. Boie. Capacitive impedance readout tactile image sensor. In *Proc. 1st IEEE Computer Society Int. Conf. on Robotics*, pages 370–379, March 1984.

[Dar89] P. Dario. Tactile sensing for robots: present and future. *The Robotics Review 1*, pages 133–146, 1989.

[FB91] R. S. Fearing and T. O. Binford. Using a cylindrical tactile sensor for determining curvature. *IEEE Trans. Robotics and Automation*, v. 7:806–817, 1991.

[FDB88] A. S. Fiorillo, P. Dario, and M. Bergamasco. Sensorized robot gripper. *Robotics*, v. 4, n. 1:49–55, Mar 1988.

[Fea90] R. S. Fearing. Tactile sensing mechanisms. *Int. J. Robotics Research*, v. 9, n. 3:3–23, 1990.

[GT89] Steven J. Gordon and William T. Townsend. Integration of tactile-force and joint-torque information in a whole-arm manipulator. In *IEEE Int*

Conf Rob Autom, volume vI (of 3), pages 464–469, Intelligent Autom Syst Inc, Cambridge, MA, USA, 1989. IEEE, IEEE Service Center, Piscataway, NJ, USA.

[HC92] R. D. Howe and M. R. Cutkosky. Touch sensing for robotic manipulation and recognition. *The Robotics Review 2*, pages 55–112, 1992.

[Hil82] W. D. Hillis. Active touch sensing. *International Journal of Robotics Research*, v. 1, n. 2:33–44, Summer, 1982.

[JMBP88] S. C. Jacobsen, I. D. McCammon, K. B. Biggers, and R. P. Phillips. Design of tactile sensing systems for dextrous manipulators. *IEEE Control Systems Magazine*, v. 8, n. 1:3–13, 1988.

[JZH96] D. Johnston, P. Zhang, and J.M. Hollerbach. An full tactile sensing suite for dextrous robot hands and use in contact force control. In *IEEE International Conference for Robotics and Automation*, pages 1286–1291, April 1996.

[Lee92] Sukhan Lee. Distributed optical proximity sensor system: Hexeye. In *Proceedings - IEEE International Conference on Robotics and Automation*, volume (IEEE cat n 92CH3140-1). v. 2, pages 1567–1572, Jet Propulsion Lab, California Inst of Technol, Pasadena, CA, USA, 1992. IEEE, IEEE Service Center, Piscataway, NJ, USA.

[LH91] Sukhan Lee and Hernsoo Hahn. Recognition and localization of 3-d natural quadric objects based on active sensing. In *Proceedings - IEEE International Conference on Robotics and Automation*, volume (91CH2969-4). v. 1, pages 156–161, Jet Propulsion Lab, California Inst of Technol, Pasadena, CA, USA, 1991. IEEE, IEEE Service Center, Piscataway, NJ, USA.

[McC90] I. D. McCammon. *Tactile Sensing for Dextrous Robot Hands*. PhD thesis, Dept. Mechanical Engineering, University of Utah, 1990.

[MJ90] I. D. McCammon and S. C. Jacobsen. *Tactile sensing and control for the Utah/MIT hand.* Springer-Verlag, NY, 1990.

[NF92] J. L. Novak and J. T. Feddema. A capacitance-based proximity sensor for whole arm obstacle avoidance. In *Proceedings - IEEE International Conference on Robotics and Automation*, volume (IEEE cat n 92CH3140-1). v. 2, pages 1307–1314. IEEE, IEEE Service Center, Piscataway, NJ, USA, 1992.

[PB96] G. Petryk and M. Buehler. Dynamic object localization via a proximity sensor network. In *IEEE/SICE/RSJ Int. Conf. Multisensor Fusion and Integration for Intelligent Systems*, pages 337–341, Dec 1996.

[PJ81] J. R. Phillips and K.O. Johnson. Tactile spatial resolution. ii. neural representation of bars, edges, and gratings in monkey primary afferents. *J. Neurophysiol.*, v. 46:1192–1203, 1981.

[PMYT92] Emil M. Petriu, William S. McMath, Stephen S.K. Yeung, and Niculaie Trif. Active tactile perception of object surface geometric profiles. *IEEE Transactions on Instrumentation & Measurement*, v. 41, n. 1, Feb 1992.

[RK89] Rocky R. Reston and Edward S. Kolesar. Pressure-sensitive field-effect transistor sensor array fabricated from a piezoelectric polyvinylidene fluoride film. In *Proceedings of the Annual Conference on Engineering in Medicine and Biology*, volume v. 11, pt. 3, pages 918–919, US Air Force Inst of Technol, Dep of Electr & Comput Eng, Dayton, OH, USA, 1989. Alliance for Engineering in Medicine & Biology, Bethesda, MD, USA. Available from IEEE Service Cent (cat n 89CH2770-6), Piscataway, NJ, USA.

[RM90] N. I. Rafla and F. L. Merat. Vision-taction integration for surface representation. In *IEEE International Conference on Systems Engineering*, Aug 1990.

[RVB93] Dominiek Reynaerts and Hendrik Van Brusse. Two-fingered full envelope dexterous manipulation. In *Proceedings - IEEE International Conference on Robotics and Automation*, volume v. 2, pages 436–441, Katholieke Univ Leuven, Heverlee, Belg, 1993. IEEE, IEEE Service Center, Piscataway, NJ, USA.

[SA94] Hiroyuki Shinoda and Shigeru Ando. Ultrasonic emission tactile sensor for contact localization and characterization. In *IEEE International Conference on Robotics and Automation*, pages 2536–2543, Univ of Tokyo. Tokyo, Jpn, 1994. IEEE Service Center, Piscataway, NJ, USA. pt 3.

[SGH86] D. M. Siegel, I. Garabieta, and J. M. Hollerbach. An integrated tactile and thermal sensor. In *IEEE International Conference for Robotics and Automation*, pages 1286–1291, April 1986.

[SM] Jeffrey S. Schoenwald and Jim F. Martin. Fiber optic tactile sensor for robot grippers. Technical report, Technical Paper - Society of Manufacturing Engineers, Rockwell Int Science Cent, Thousand Oaks, CA, USA.

[Spe90] T. Speeter. A tactile sensing system for robotic manipulation. *International Journal of Robotics Research*, v. 9, n. 6:25–36, December 1990.

[UR92] Jean-Pierre Uldry and R. Andrew Russell. Developing conductive elastomers for applications in robotic tactile sensing. *Advanced Robotics*, v. 6, n. 2:255–271, 1992.

[Vra] John M. Vranish. *Magnetoinductive Skin for Robots.* IFS Publ Ltd, Kempston, Engl, & Springer-Verlag, Heidelberg, West Ger & New York, NY, USA, NBS, USA.

[XHM95] Y. Xu, J. M. Hollerbach, and D. Ma. A nonlinear PD controller for force and contact transient control. *IEEE Control System*, v. 15, n. 1:15–21, 1995.